THE JOURNAL OF PHYSICAL CHEMISTRY LETTERS
A JOURNAL OF THE AMERICAN CHEMICAL SOCIETY

pubs.acs.org/JPCL

Mini-Review

Molecular and Supramolecular Materials: From Light-Harvesting to Quantum Information Science and Technology

Yipeng Zhang, Catrina P. Oberg, Yue Hu, Hongxue Xu, Mengwen Yan, Gregory D. Scholes,* and Mingfeng Wang*

Cite This: *J. Phys. Chem. Lett.* 2024, 15, 3294−3316

Read Online

ACCESS | Metrics & More | Article Recommendations

ABSTRACT: The past two decades have witnessed immense advances in quantum information technology (QIT), benefited by advances in physics, chemistry, biology, and materials science and engineering. It is intriguing to consider whether these diverse molecular and supramolecular structures and materials, partially inspired by quantum effects as observed in sophisticated biological systems such as light-harvesting complexes in photosynthesis and the magnetic compass of migratory birds, might play a role in future QIT. If so, how? Herein, we review materials and specify the relationship between structures and quantum properties, and we identify the challenges and limitations that have restricted the intersection of QIT and chemical materials. Examples are broken down into two categories: materials for quantum sensing where nonclassical function is observed on the molecular scale and systems where nonclassical phenomena are present due to intermolecular interactions. We discuss challenges for materials chemistry and make comparisons to related systems found in nature. We conclude that if chemical materials become relevant for QIT, they will enable quite new kinds of properties and functions.

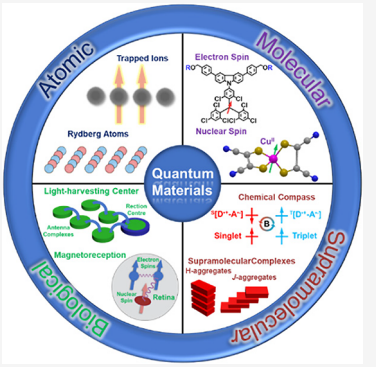

Quantum information and quantum computing have been developing rapidly in various fields. The applications of quantum information technology (QIT) are generally categorized into three main fields: quantum computation, quantum information processing, and quantum sensing. Quantum computation employs qubits and principles of quantum mechanics significantly accelerating certain calculations.[1−8] Quantum computers can solve certain kinds of "NP-hard" algorithms (i.e., algorithms that cannot work in polynomial time) faster than classical computers. Quantum computers today still have a limited number of qubits, with a recent paper reporting a 127-qubit processor using 60 layers of quantum gates.[9] Increasing the number of qubits leads to a speedup of computation time relative to classical computers, although there is still progress to be made to increase quantum computing capabilities. Quantum information uses entanglement to transmit information in a secure way.[1,10−14] Quantum sensing utilizes the high sensitivity of coherent quantum systems to the external environment to enhance measurement.[15−17] A variety of materials such as ion traps,[18−23] electronic[7,24−35] and nuclear spins,[8,36−43] quantum dots,[44−48] and superconducting circuits[6,49−51] have been studied as qubits for QIT. Are there opportunities for chemical materials that could facilitate QIT?

Materials chemistry combines molecular building blocks in sophisticated multiscale organization. There is an incredible range of systems that have structure on many scales. The size, complexity, and relatively weak interactions among building blocks limit the relevance of chemical materials for current QIT applications. But are there new opportunities offered by these systems, especially for fundamental study of quantum phenomena in large and disordered systems? It is perhaps too early to answer this question with compelling examples. Instead we explore what we know so far.

QIT has been focused on platforms where robust entangled states can be produced with high fidelity, transmitted, processed, and decoded. Less progress has been made in working out how to characterize and exploit quantum correlations that might be present in complex molecular systems.[12] Recent studies have been directed to strongly correlated solid-state systems known as quantum materials. Here we examine chemical systems that are, in general, weakly correlated. We aim to contribute some perspectives on their main characteristics that might provide opportunities in quantum information science. To help reach a broad readership, we begin with a basic review of concepts. We then discuss examples that are grouped into two themes: (i) systems where nonclassical function is observed on the

Received: January 26, 2024
Revised: March 1, 2024
Accepted: March 11, 2024
Published: March 18, 2024

https://doi.org/10.1021/acs.jpclett.4c00264
J. Phys. Chem. Lett. 2024, 15, 3294−3316

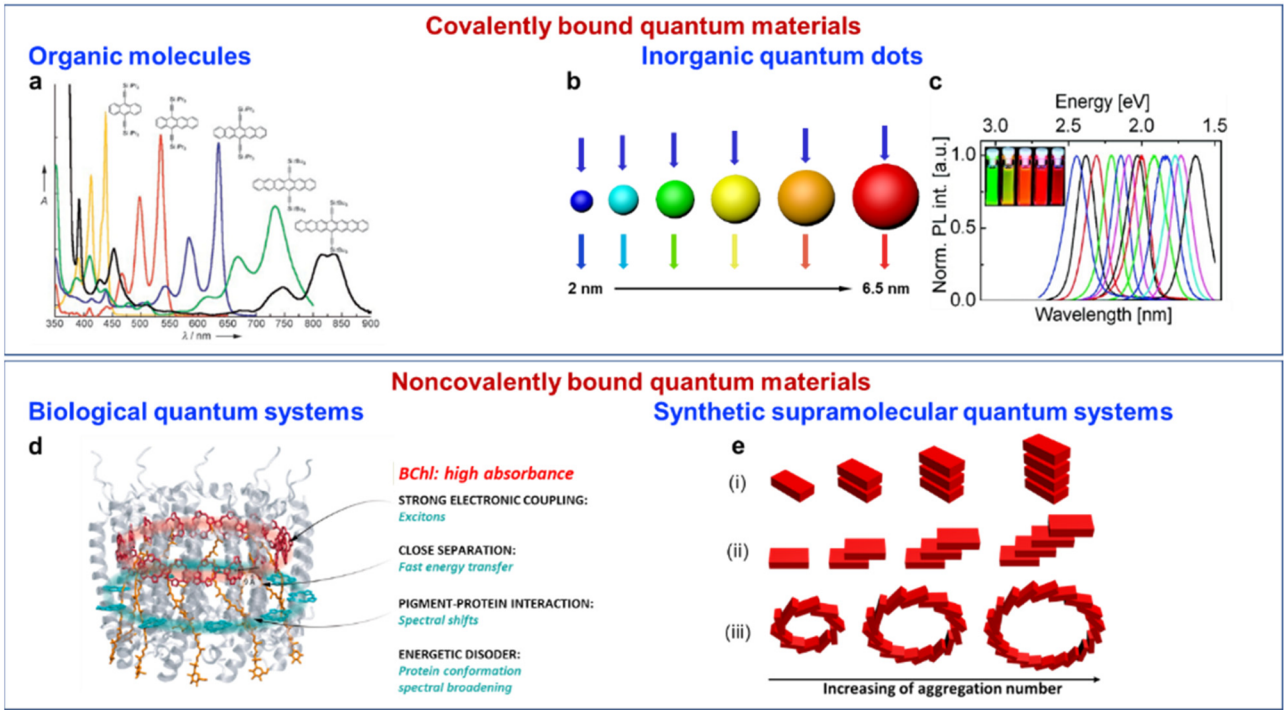

Figure 1. Representative diagram of different types of quantum materials. (a) UV−vis absorption spectra of series functionalized acenes. Adapted with permission from ref 55. Copyright 2008 Wiley-VCH. (b) Schematic diagram and (c) normalized photoluminescence spectrum of quantum dots.[62,63] Adapted with permission from ref 63. Copyright 2007 American Chemical Society. (d) The LH complexes of purple bacteria illustrate phenomena affecting excitation energy transfer. Adapted with permission from ref 74. Copyright 2017 American Chemical Society. (e) Schematic presentation of three synthetic supramolecular quantum systems associated by noncovalent interaction among molecular chromophores: (i) classical H-aggregate; (ii) classical J-aggregate; (iii) cyclic coulomb coupled J-aggregate.[84]

molecular scale; (ii) systems where nonclassical phenomena are present because of intermolecular interactions.

The advances in quantum mechanics during the early 20th century have not only revolutionized the creation of new materials through a bottom-up synthetic approach but also offered a rationale for the structure−property relationship of materials across different length scales ranging from subatomic to atomic to molecular levels and beyond.[52] Specifically, at a molecular level, one could precisely tune the optical band gap of acenes by controlling the number of fused benzene rings (Figure 1a).[53−55] Similar size-dependent properties have also been observed in quantum dots (QDs), so-called artificial atoms, as benchmarks of quantum materials (Figure 1b). QDs are semiconductor particles on a nanometer scale with unique size-dependent optical and electronic properties due to the quantum confinement effect.[45,56−61] Typical photoluminescence (PL) spectra of size-selected fractions of thioglycolic- and mercaptopropionic-capped CdTe nanocrystals as QDs are shown in Figure 1c.[62,63] The PL of QDs can be tuned from 500 to 700 nm by decreasing their diameter. The narrow and tunable PL and tunable spin states of QDs have enabled their applications not only in bioimaging[46,64] and light-emitting diodes (LEDs)[65−67] but also as single-photon sources[68,69] and as qubits in gate-defined devices.[70−73]

Molecular aggregates and assemblies enable more elaborate tuning of photophysical properties.[74] Photosynthesis takes place in light-harvesting (LH) complexes (Figure 1d), which are highly optimized through thousands of years of evolution. A notable characteristic of these natural systems is the way molecules are exquisitely organized in a structural framework. LH complexes from purple bacteria, for example, are comprised of carotenoid and bacteriochlorophyll chromophores that absorb light in the green and far-red light of wavelengths above 750 nm.[74−76] On the one hand, LH2 (also termed B800−B850) has a characteristic circular nonamer (or octamer) structure consisting of nine (or eight) subunits and absorption peaks at ∼850 and 800 nm, respectively. On the other hand, LH1, with a larger aggregation number with 16-fold symmetry, shows a single peak at 875 nm. Such intricate and functional structures remain beyond the reach of the present synthetic supramolecular systems.

Several types of aggregates, including *J*-, *H*-, *X*-aggregate and aggregate-induced emission (AIE), composed of synthetic organic chromophores, have been intensively studied, and intermolecular interactions dictate nonclassical phenomena and collective properties.[77−79] In synthetic systems, some dye aggregates or supramolecular polymers present significant scale-dependent optical properties similar to nature. With increasing aggregation size or supramolecular degree, the absorption or emission of chromophores may become narrower and red-shifted while the nonradiative rate should decrease quickly according to the computational chemistry.[80−83] Figure 1e illustrates three typical aggregate classifications: (i) classical *H*-aggregate, (ii) classical *J*-aggregate, and (iii) cyclic Coulomb coupled *J*-aggregate.[84] For typical H-aggregate (i), a larger aggregation number always leads to a hypsochromic shift in absorption peaks and suppressed fluorescence relative to the monomer.[84] However, for classical *J*-aggregate (ii), the dyes are arranged in a slip-stack arrangement with a slip angle <54.7°[85] and a narrower and bathochromic shifted absorption peak with a stronger absorption coefficient. One of the exceptions in *J*-aggregates

https://doi.org/10.1021/acs.jpclett.4c00264
J. Phys. Chem. Lett. 2024, 15, 3294−3316

is cyclic Coulomb coupled *J*-aggregate (iii) found in LH complexes. The dyes are also aggregated in a cyclic or tubular slip-stacked manner similar to that in nature. Nevertheless, the unique topology and the direction of the dipole moment in cyclic Coulomb coupled *J*-aggregate do not lead to the narrow absorption and increased fluorescence decay rate as observed in other types of *J*-aggregates.[84,86−89] But after natural evolution, these types of aggregates all have been optimized to harvest sunlight and transfer energy to the reaction center at high efficiency.

Herein, we review recent advances in quantum materials across molecular and supramolecular (or intermolecular) scales. We describe some representative systems on each scale and discuss opportunities for future work. In consideration of many excellent reviews on atomic quantum materials,[90−94] molecular quantum materials,[10,12,32,95,96] quantum biology,[74,97,98] and QIT,[2,15,99−105] the present review mainly focuses on quantum systems at molecular and supramolecular scales, especially radicals, nuclear spins, and bioinspired quantum systems, as well as systems where intermolecular interactions cause nonclassical phenomena. The challenges of existing quantum materials and the advantages of synthetic supramolecular materials over conventional materials for QIT are also discussed.

Here we include a very brief overview of some key points about quantum information science. In other papers, we provide a more detailed tutorial review.[106] Quantum systems considered model qubits are typically two-level systems. The classical analogy is a switch that can take values of 0 or 1, just like the binary basis for digital communication and computation, which are based on two-state systems. A system containing n classical switches can encode 2^n different classical states.

Qubits are states in two-dimensional Hilbert space, that is, vectors comprising the basis states $|0\rangle$ and $|1\rangle$. In a system of n qubits, states inhabit a space that is constructed from the tensor product of the Hilbert spaces of each qubit in our system. If every qubit were to be definitively set in either the $|0\rangle$ or $|1\rangle$ state, like the classical switches, then we obtain 2^n unique product states in $\mathcal{H}$, very much like we did for the classical system of switches. This set of product states forms one possible basis for our general quantum (pure) states to be found in the Hilbert space $\mathcal{H}$.

More general states are generated by taking the superpositions of the product states. These are especially interesting states because they have no classical counterpart. What makes these states special is that they have properties that cannot be exhibited by any classical system, properties epitomized by entanglement and nonlocality. These quantum correlations generally come hand-in-hand with strong classical correlations. For example, consider one of the famous Bell states:

$$\Psi_+ = \frac{1}{\sqrt{2}}[|0\rangle_A|1\rangle_B + |1\rangle_A|0\rangle_B]$$

$$\Psi_- = \frac{1}{\sqrt{2}}[|0\rangle_A|1\rangle_B - |1\rangle_A|0\rangle_B]$$

$$\Phi_+ = \frac{1}{\sqrt{2}}[|0\rangle_A|0\rangle_B + |1\rangle_A|1\rangle_B]$$

$$\Phi_- = \frac{1}{\sqrt{2}}[|0\rangle_A|0\rangle_B - |1\rangle_A|1\rangle_B]$$

Say, Ψ_+, where we do not know whether subsystem A, or B, is in the 0 or 1 state. But we do know that if A is 0, the B is 1, and vice versa. That is a classical correlation. However, more sophisticated pairs of measurements resolve quantum correlations that come about because of how the states are constructed in Hilbert space and thus account for the wave-basis of quantum mechanics. A physical example is interference, as seen in the double-slit experiment. Obviously, interference evidences wave-like properties, but the phenomenon is shared by classical and quantum systems. The purely quantum wave-like properties are uncovered by higher-order correlations.[107]

It is not obvious at first glance how to understand the extra information in a quantum system compared with an analogous classical system. For example, n classical switches (two-level systems) can encode 2^n distinct binary numbers, which is the same as the size of the quantum state space. The maximum amount of information encoded in either case is the same. One quantum advantage for conveying information comes from using compression strategies that are only available to quantum systems. While one qubit does not convey more information than one classical bit, the quantum correlations in an entangled system can be exploited to enable information to be more compressed, allowing quantum communication channels to have greater capacity than comparable classical channels.[1] A second advantage is that quantum mechanical laws can be leveraged to make communication more secure, such as in quantum cryptography.[108] Another way to view potential advantages obtainable from quantum systems lies in how states are constructed, whereby it takes only a linear number of classical resources to construct an exponentially large superposition.

Besides qubits on the atomic scale,[22,23,94,109−111] molecular qubits have shown impressive characteristics, such as long spin coherence,[29] maneuverable triplet states,[112] and organic molecules with spin-singlet.[40] Chemistry offers a bottom-up design and synthetic[7] approach that enables tunability, control, and scalability of qubits via chemical reactions of extended structures and compatibility across different environments.[13] Thus, molecular qubits can be well controlled over complex intrinsic and extrinsic environments.

Quantum sensing refers to the use of quantum resources, such as coherence or entanglement, to measure a physical property that may be quantum or classical in nature, typically with higher sensitivity than classical sensors.[15] Experimentally, it is important to evaluate and recognize the sensitivity of the sensor, as well as the physical parameter(s) that the sensor responds to. There are two parameters that are key to evaluating the performance of qubits for quantum sensing and computing: spin−lattice relaxation time (T_1) and coherence time (T_m).[95] T_1 represents the time it takes for an excited spin population to relax to the ground state, while T_m represents the lifetime of the quantum superposition state. In addition, the physical parameters that the quantum sensors detect include spin-based systems (like nuclear spins and electron spins), which respond to magnetic fields, or charged systems (like ion-traps), which respond to electric fields.

Here, we present some examples of experimental implementations of quantum sensors in materials-based systems, such as the use of molecular spins, as well as applications of quantum information technology from biology and bioinspired materials. These systems have nonclassical functions that are observed on the molecular scale.

https://doi.org/10.1021/acs.jpclett.4c00264
J. Phys. Chem. Lett. 2024, 15, 3294−3316

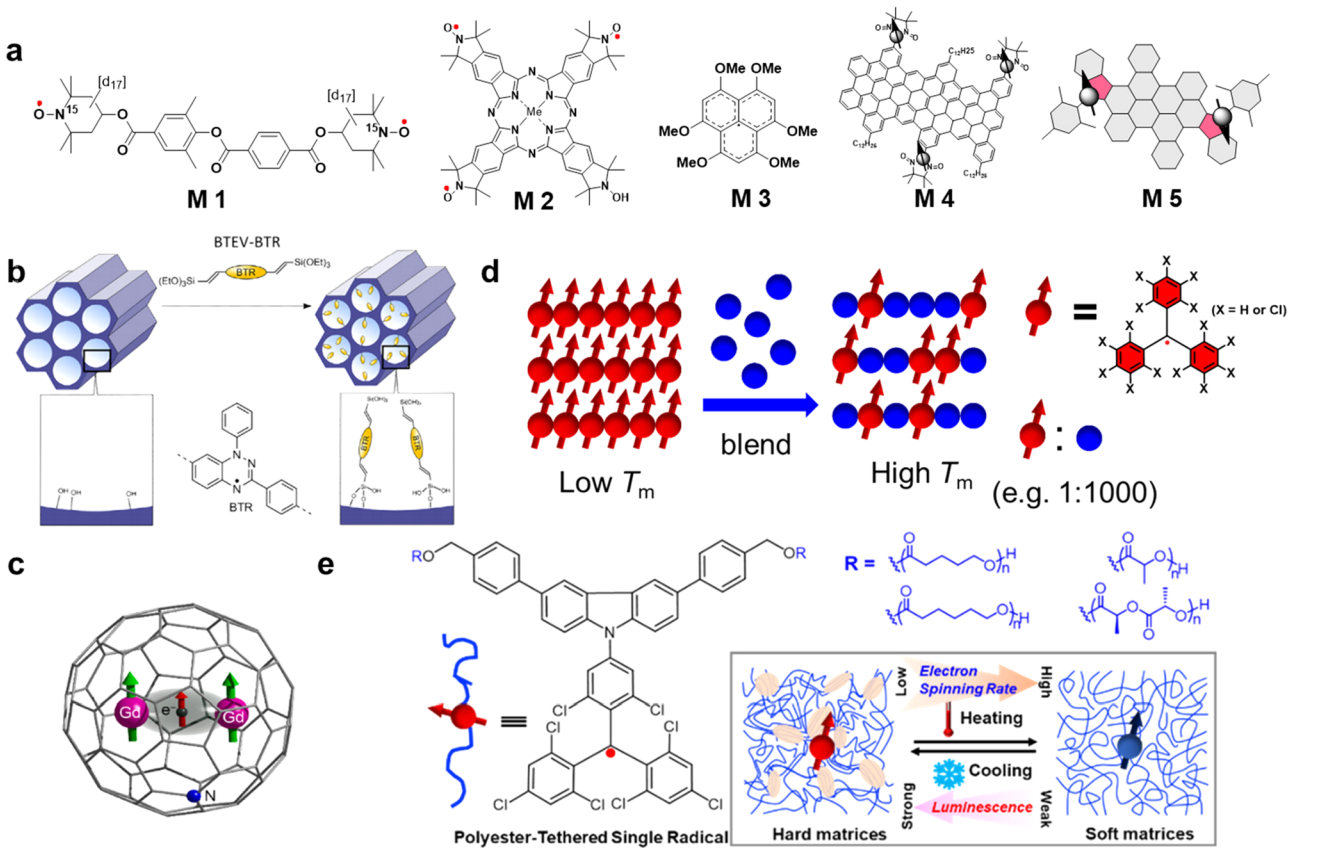

Figure 2. Molecular quantum materials and technologies. (a) Synthetic electron spin systems, M1: (2,2,6,6-tetramethylpiperidin-N-oxyl-4-yl) 3,5-dimethylbenzoate-4-yl tetrephthalate diradicals;[32] M2: magnesium phthalocyanine with three nitroxyl radicals;[32] M3: Hexamethoxyphenalenyl radical;[32] M4: side-functionalized graphene nanoribbon radicals;[123] M5: topological stabilized magnetic centers.[123] (b) Schematic representation of the grafting procedure leading to immobilized BTR radicals inside the pores of SBA-15 host phase.[34] Adapted with permission from ref 34. Copyright 2021 Wiley-VCH. (c) Molecular structure of two GdIII trapped in a C79N fullerene.[95] Adapted with permission from ref 95. Copyright 2017 American Chemical Society. (d) TM radicals doped with their corresponding diamagnetic hydrogenated products to increase Tm.[132] (e) Schematic presentation of the impact of polymer rigidity on the luminescence and electron spin dynamics of the radical polymers.[35]

Several physical realizations of qubits have been investigated, among which the use of electronic or nuclear spins has attracted considerable interest. Spin is intrinsically a two-level quantum system that can easily be manipulated by electromagnetic radiations and detected by magnetic resonance techniques.[113] Moreover, through the controllability of chemical synthesis, molecular spins can be created in arrays of one-, two-, and three-dimensional architectures[33,39,114] and can be integrated with electronic and photonic devices.[26,115] We start by discussing the use of electron spins as qubits for quantum information processing.

The use of electron spins as qubits is instinctive since the spin up and down states mimic the well-defined qubit states $|0\rangle$ and $|1\rangle$ and is advantageous due to the scalability of these molecular systems.[32] However, decoherence caused by environmental interactions (electromagnetic fields, phonons, or impurities), spin−spin interactions, and spin−orbit coupling limits the coherence times of electron spins. Some strategies, such as spin isolation and low-temperature operation techniques, as detailed below, have been developed to improve the coherence time. Here, we consider the use of radicals as electron spins for hosting spin qubits in materials systems for quantum sensing.

Figure 2a shows some representative examples of organic spin qubits. Although most molecules with unpaired spins are unstable, some of them, such as some nitrogen-based radicals (M1, M2 in Figure 2a), can operate under relatively mild conditions.[32,116] Nitroxyl molecules are stable by coupling electron spins with signature ^{14}N, making them an important probe for electron paramagnetic resonance (EPR) spectroscopy.[117] Because they are easily modified and characterized by nuclear magnetic resonance (NMR), Takui and co-workers have done systematic work on nitroxyl radicals in single- and multiqubit molecules.[24,25,28,36,116,118,119] The biradical (2,2,6,6-tetramethylpiperidine-oxyl-4-yl)-3,5-dimethylbenzoate-4-yl terephthalate (M1) was reported as a molecular system to perform quantum gating,[12] where the 3,5-dimethylbenzoate-4-yl group was applied to link two nitroxyl radicals. The two well-defined single spins in M1 are weakly coupled, and the *g*-tensors at the N−O sites of the tetramethylpiperidine-1-oxyl (TEMPO) groups are nonequivalent as the principal axes point in different directions. The distance between N−O from the TEMPO group is designed as 2.0 nm, which is about 10 MHz of electron spin dipolar interaction.

A magnesium phthalocyanine with three nitroxyl radicals on the periphery (M2) was first reported for adiabatic quantum computing.[28,32] EPR/NMR pulse sequences were executed to manipulate quantum gate operations in open-shell M2 molecular entities. The pulse sequences showed higher computing speed with stronger spin interactions, especially electron spins, demonstrating the advantages and possibilities of molecular spin quantum simulators.

https://doi.org/10.1021/acs.jpclett.4c00264
J. Phys. Chem. Lett. 2024, 15, 3294−3316

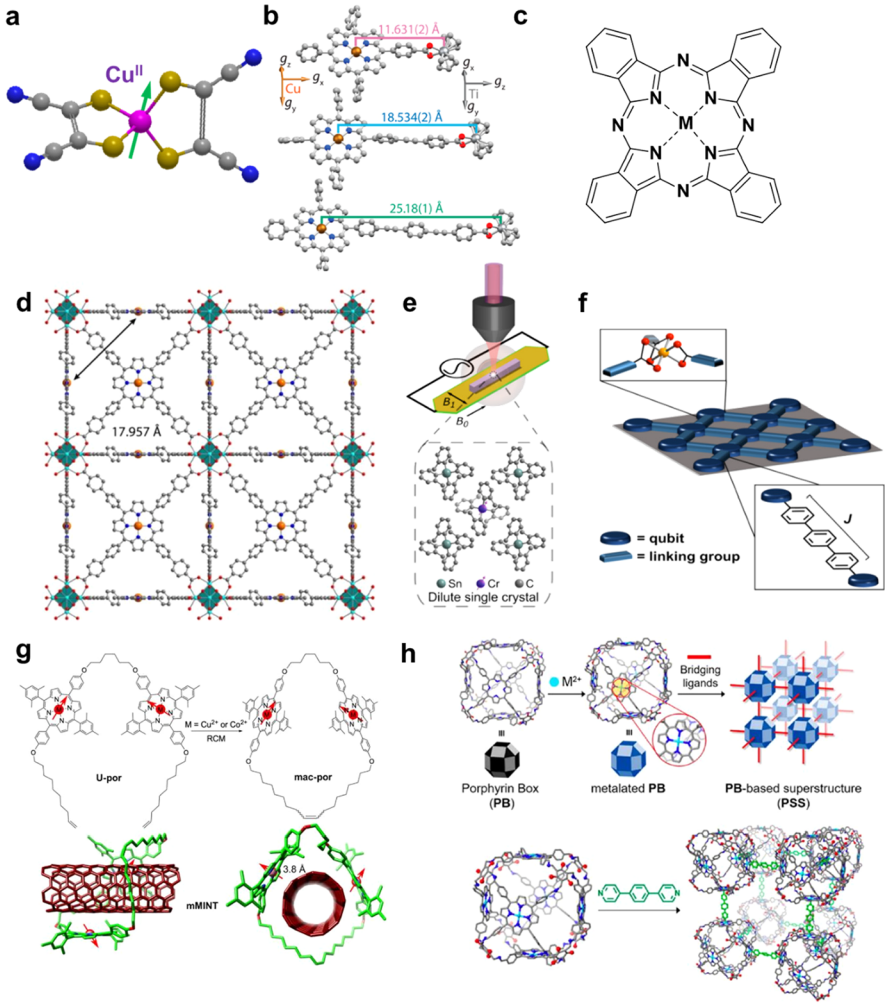

Figure 3. (a) A paramagnetic metal complex with long spin coherence (Color code: gray, C; green, Si; yellow, S; blue, N.).[95] (b) Single-crystal X-ray structures of bimetallic porphyrin complexes.[135] Adapted with permission from refs 95 and 135. Copyright 2021 American Chemical Society. (c) Copper phthalocyanine molecule.[136] (d) Crystal structure of Zr−Cu−NU-1102 with each porphyrinic ligand metalated with Cu^{2+}. Gray, orange, blue, and red represent carbon, copper, nitrogen, and oxygen, respectively. Zr 6 nodes are represented by turquoise polyhedral. Nearest Cu−Cu distances are highlighted. Structures were obtained from previously published works.[43] Adapted with permission from ref 43. Copyright 2020 American Chemical Society. (e) Schematic diagram of optical excitation and photoluminescence collection for spin initialization and readout.[13] Adapted with permission from ref 13. Copyright 2020 AAAS. (f) Schematic diagram of an array of surface quits, showing potential link and metal complex geometry. J indicates the strength of magnetic coupling between the qubits.[137] Adapted with permission from ref 137. Copyright 2017 American Chemical Society. (g) A ring-closing metathesis turned the open porphyrin-based macrocycle (U-por) into the porphyrin macrocycle (mac-por) around the single-wall carbon nanotube. The final magnetic MINT (mMINT) structures were obtained by density functional theory (DFT) calculations.[8] Adapted with permission from ref 8. Copyright 2021 American Chemical Society. (h) Concept behind the realization of hierarchical superstructures based on metalated-porphyrin boxes (top) and practical realization using Zn-porphyrins and dipyridyl terminated bridging ligands (bottom).[139] Adapted with permission from ref 139. Copyright 2018 American Chemical Society.

Takui, Morita, and co-workers have also reported graphite-like fragments of stable organic radicals.[120−122] By applying six methoxy groups to a neutral carbon-centered π radical (M3 in Figure 2a), they investigated quantum spin simulators for a large number of interacting spins in molecular frames, the quantum coherence of which arose from rotational motions of the interacting nuclear spins with a delocalized electron in the core.

Another example of graphene-based molecular spins is M4 in Figure 2a.[123] Such graphene lattices can fuse rings in an sp^2 framework,[27] and bottom-up synthesis can be used to relate these structures on a large scale.[44] Upon the formation of two (1,0) dislocations, radical pairs gain the capability to traverse the network, facilitating trimming of the lattice along the graphene for the desired geometry. While these molecules have been actively investigated for applications in electronics, biology, and energy, their untapped potential in quantum devices remains an area yet to be explored.[38]

In 2019, Bogani and co-workers reported a type of molecular qubit based on a saddle-shaped diindeno-fused bischrysene (M5 in Figure 2a) with a stable structure of open-shell biradical.[123] The incomplete dehydrogenation in the final synthetic route to M5 resulted in impurities of a monoradical species that were difficult to separate because of only one single hydrogen difference. However, this monoradical impurity is useful for determining how a single pentagonal element behaves in the lattice. Although the signal from monoradical components was overshadowed by that from M5 at room temperature, the monoradiacal signal was still detectable around 100 K.[123] The room-temperature EPR

https://doi.org/10.1021/acs.jpclett.4c00264
J. Phys. Chem. Lett. 2024, 15, 3294−3316

results showed signals of delocalized unpaired electrons, indicating weak dipolar and hyperfine coupling. With the decrease of temperature from room temperature to 5 K, T_1 of M5 in powders or the solid state can increase from 1 to 100 μs, while T_m of M5 increased from ca. 300 ns in the solid state to 28 μs at 80 K in solution of CS_2 as the solvent. Decoherence may be aroused by electron−electron scattering along π-stacks in the system, so a new synthetic route to explore may be to eliminate π-stacking in solid-state materials for an increased coherence time.

To enhance the stability of such molecular qubits under ambient conditions, Froba, Fedin, and co-workers[34] proposed a strategy to embed radicals into mesoporous silica frameworks with room-temperature coherence times over 2 times higher than those in metal complexes (Figure 2b). Mesoporous silica hosts (Santa Barbara Amorphous-type material, SBA-15) with cylindrical pores with diameters of 9.1 nm were combined with 0−20% weight loading of the Blatter-type bis-(triethoxysilylvinyl)triazinyl radical (BTEV-BTR) precursor as a source of paramagnetic spin centers. For the radical precursor, the isotropic hyperfine interaction (HFI) constant of three ^{14}N nuclei can be well simulated by the CW EPR spectrum, which agrees with previous studies of Blatter-type radicals.[30,42,124,125] Additionally, the EPR spectra of different radical loading ratios appeared similar to that of unloaded radicals at 80 K; there was a decrease in both T_1 and T_m with increasing radical loading ratios, implying that spin−spin interactions between radicals play a profound role in overall relaxation. Finally, quantum operations were demonstrated to be successfully performed with a Rabi oscillation experiment,[126] where a single microwave pulse with variable length is applied to flip the electron magnetization. The feasibility of spin manipulation was confirmed by the linear dependence of the oscillation frequencies on the magnitude of the microwave field. This synthetic approach is promising for tuning the properties of molecular qubits at room temperature.

To minimize external environmental noise, spins can also be encapsulated into fullerenes, such as $Gd^{III}@C_{79}N$[95] (Figure 2c), $^{14}N@C_{60}$,[127,128] and $^{31}P@C_{60}$.[129] The cages of fullerenes can be designed to stabilize the electron spin generated inside the cage. As a consequence, coherence times of 1.6 μs at 5 K can be observed in an environment almost free of nuclear spins, although these coherence times are not adequately long enough to satisfy T_m > 100 μs and ultralow temperature is still required.[130]

Finally, π-conjugated organic semiconductors show promise as materials for quantum information processing. For example, triphenylmethyl (TM) radicals and its derivatives exhibit long T_1 up to 35.6 μs and T_m up to 1.08 μs under ambient conditions after being doped with their corresponding diamagnetic hydrogenated products with a molar fraction of 99.9% (Figure 2d).[131,132] Room-temperature quantum coherence and Rabi cycles in thin films were observed with the TM derivatives. By designing energy resonance between emissive doublet and triplet levels, tris(2,4,6-trichlorophenyl) methylcarbazole radicals covalently coupled with anthracene presented both efficient luminescence and near-unity generation yield of excited states with spin multiplicity S > 1.[133] Recently, Wang's group reported a series of polyester-tethered TM radicals with tunable luminescence and electron spin resonance (Figure 2e).[35] By ring-opening polymerization from a carbazole-substituted TM, four representative polyesters [poly(δ-valerolactone), poly(ε-caprolactone), poly(D, L-Lactide), and poly(L-lactide)] were synthesized to suppress interradical aggregation. The rigidity of the polymeric matrices significantly affects the PL and electron spin resonances in solid states. Polymers with high glass-transition temperature (T_g) lead to stronger photoluminescence intensity with longer lifetime and longer electron spin correlation time, which offers a new method to control the PL in light-emitting devices and coherence for quantum information processing.[134]

Chemical design offers boundless possibilities to exploit the electron or nuclear spins of magnetic molecules (Figure 3a). Nuclear spins on magnetic molecules, compared to NV centers in diamond and phosphorus impurities in silicon, offer competitive advantages on their precise structural control at a molecular level and ease of scalability. Another appealing advantage of nuclear spins is from suppression of decoherence. Compared to electron spins, nuclear spins are more robust against the collapse of the superposition state caused by environmental perturbations. Despite these advantages, nuclear spins as qubits still face challenges such as the lack of tunability and difficulty in switching interactions between them.[95] Scaling-up of such qubits has also been limited by the difficult connection of two nuclear spins located at different molecules, on account of their small magnetic moments and their weak coupling to electromagnetic radiation. However, there are several promising systems in which nuclear spins can be exploited for use as spin qubits.

Porphyrins and phthalocyanines are among the most studied families specifically designed for applications on quantum information and spintronics. Magnetic porphyrins have been preferable qubit candidates due to their relatively long coherence times[39] and magnetic properties.[41] Transition metal-based porphyrin complexes (Figure 3b) with different spatial distances (from 1.2 to 2.5 nm) between Cu^{2+} and Ti^{3+} were synthesized, and the coherence times were measured by EPR spectroscopy.[135] The coherence times are dominated by intramolecular rather than intermolecular spin−spin interactions. Thin films of paramagnetic copper phthalocyanine (CuPc; Figure 3c) dispersed in diamagnetic matrices of free-base H_2Pc have been reported as possible candidates for quantum information processing, with decoherence times of 2.6 μs at 5 K.[136] In addition, organic molecules have relatively weak spin−orbital coupling, resulting in large Hilbert space with nondegenerate transitions, which can be further customized by chemical modifications.

Metal−organic frameworks (MOFs) have attracted a lot of research interest as quantum sensing materials because they can force molecular qubits into precise arrays. One approach is to make use of Cu porphyrins that self-assemble into 2D molecular networks on surfaces or into MOFs. Freedman and co-workers synthesized expanded Cu-porphyrin MOFs with an increased qubit−qubit distance (Figure 3d). The increased qubit−qubit distance can reduce spin−spin interactions and induce improved quantum coherence times and the observed recovery time.[43]

Optically addressable molecular spin qubits have been synthesized (Figure 3e), which can be initialized and read out with light and manipulated with microwave fields.[13] Encapsulating a metal ion with an electronic spin inside organic moieties as ligands forms well-defined qubit systems with synthetic tunability. By applying a strong ligand-field environment, a spin-singlet (S = 0) is the lowest-lying electronic excited state, making the optical readout possible since a probed spin sublevel (e.g., $|0\rangle$) leads to enhanced

https://doi.org/10.1021/acs.jpclett.4c00264
J. Phys. Chem. Lett. 2024, 15, 3294−3316

photoluminescence (PL) relative to another spin sublevel (e.g., $|\pm1\rangle$). Additionally, selective excitation along with spontaneous emission cause optical polarization of the ground-state spin and result in population transfer from the probe to other spin sublevels.[31] Significantly, the relaxation time of ground-state spin should be much longer than the excited-state lifetime to accumulate spin polarization in multiple excitation and emission cycles. With a bottom-up qubit design strategy, three Cr^{4+} compounds were synthesized by differing the placement of CH_3 on the coordinating ligands.[13] The results of optically detected magnetic resonance (ODMR) demonstrate robust optical initialization, microwave spin manipulation, and optical readout of these qubit systems and show that low-symmetry structures tend to be more resistant to noise.

Another approach to designing spin-based qubits using MOFs is through a spectroelectrochemical technique where the individual molecule is directly connected to nanospaced electrodes in a transistor geometry, such as the MOFs applied in the quantum computational architecture shown in Figure 3f.[137,138] Although it is difficult to control their spatial location and synthetic process, such molecular systems not only can preserve their advantages—reproducible fabrication, extraordinary tenability, and ability to scale up—but also can be forged into solid states which bring longer coherence time to the quantum systems. Recently, Burzurí and co-workers engineered Cu^{2+} and Co^{2+} ($S = 1/2$) metalloporphyrin dimer rings mechanically bonded around carbon nanotubes (Figure 3g).[8] The design of the mechanically interlocked structure enables the interaction between spin and conduction electrons to be modulated without disturbing the molecular spin and preserving the coherence time of 25 μs.

Different from 2D networks, where the discrete structural units consist of a finite number of interacting metal ions, the hierarchical superstructure approach is considered a promising way to connect subunits. In 2018, the Kim group reported an approach by linking zinc−metalated porphyrin boxes with dipyridyl terminated bridging ligands to form hierarchical superstructures (Figure 3h).[139] Adjusting the length of the bridging ligands or adding functional groups to the ligands provides tuning of properties for selective guest encapsulation and interior functionalization, which may be useful for various applications, including quantum information processing. To further increase coherence time (T_m), a reasonable compromise between signal intensity and the T_m value should be considered.

Along with materials-based systems for quantum sensing, we can turn to biology for the presence of spin and magnetic field sensors as inspiration for future advances in the field of quantum sensing. Although the exact role of quantum mechanisms in biology remains controversial, many experiments demonstrated quantum-mechanical phenomena in biology.[140] In particular, the mixing of singlet and triplet spin states due to the close spacing of the energy levels can be used as a magnetic field sensor.

One such source of inspiration for quantum sensing is the magnetic compass of migratory birds, where there is experimental evidence supporting a mechanism that uses photopigments and coherent spin dynamics for magnetoreception. Quantum phenomena have been observed in the magnetoreception process to sense a magnetic field. Behavioral experiments excluded magnetite-based mechanisms that some organisms with a magnetic sense have no sensitivity to polarity,[141] since the operation of most magnetite-based compass models is polarity-sensitive.[142] There are several reasonable mechanisms for magnetoreception, and one of the most widely accepted mechanisms is a so-called "Radical Pair" mechanism, which involves the quantum evolution of a separated pair of electron spins supported by several experiments of spin chemistry.[143−146]

By recording the response of a European robin to the magnetic environment, the mechanism of magnetic sensing is revealed: researchers showed that these robins are sensitive to the inclination (instead of the polarization) of the magnetic field[141] and the sensor is activated by photons entering the bird's eyes.[147,148] Another analysis showed that a small oscillating magnetic field can disrupt the orientation ability of the bird and that the bird can be trained to adapt to different magnetic fields, indicating that navigation sense is strong and not dependent on a single parameter.[146,149]

Magnetosensitivity is hypothesized to arise from changes in singlet and triplet populations due to changes in the magnetic field orientation. The basic idea of the radical pair model is shown in Figure 4a. There are molecules in the eyes of birds that can absorb an optical photon and generate spatially separated electron pairs in singlet spin states independently. A singlet−triplet evolution, which depends on the inclination of the molecule affected by the Earth's magnetic field, appears because of the spatial difference between two electron spins. Recombination occurring from either a singlet or a triplet state leads to different products, which constitute a chemical signal related to the Earth's field orientation, although the specific molecule involved remains unknown.[150] The mixing of the single-triplet states enabled by an external magnetic field can be an inspiration for quantum detector designs.

Such radical pair reactions may occur within cryptochromes, which could induce visual signals because of their residence in the eyes.[144,151] The lifetime and decoherence of singlet and triplet state analysis showed that the role of these states in the radical pair mechanism is quite complicated.[150] Some dephasing experiments showed that the sensitivity of the radical pair remains intact to external fields. Since the disrupting fields were so weak, spins in the radical-pair model can maintain their quantum coherence for tens of microseconds, denoting that both coherence and entanglement properties can be sustained longer than most man-made molecular systems.[150] However, the exact mechanism of this radical pair remains elusive and warrants further study by establishing either biological or man-made models,[152,153] for example, radical pairs in which the transformation between the singlet and the triplet could be well controlled by an external magnetic field and characterized through a physical technique. The radical pair mechanism for magnetoreception in birds serves as inspiration for the design of artificial chemical sensors, particularly those that may be used for future applications to QIT.

In addition to magnetoreception, electron- and proton-tunneling in many enzymatic catalytic reactions are proven to have nuclear quantum effects.[154−156] For example, enzymes have evolved to take advantage of the quantum effect to accelerate the energy shift due to the zero-point energy. The short de Broglie wavelength of the nuclear wave function of protons makes proton-tunneling sensitive to the environment, potentially coupled with proteins, although it is still under debate.

Inspired by the avian magnetoreception system mentioned above, an artificial photochemical reaction-based magnetic

https://doi.org/10.1021/acs.jpclett.4c00264
J. Phys. Chem. Lett. 2024, 15, 3294−3316

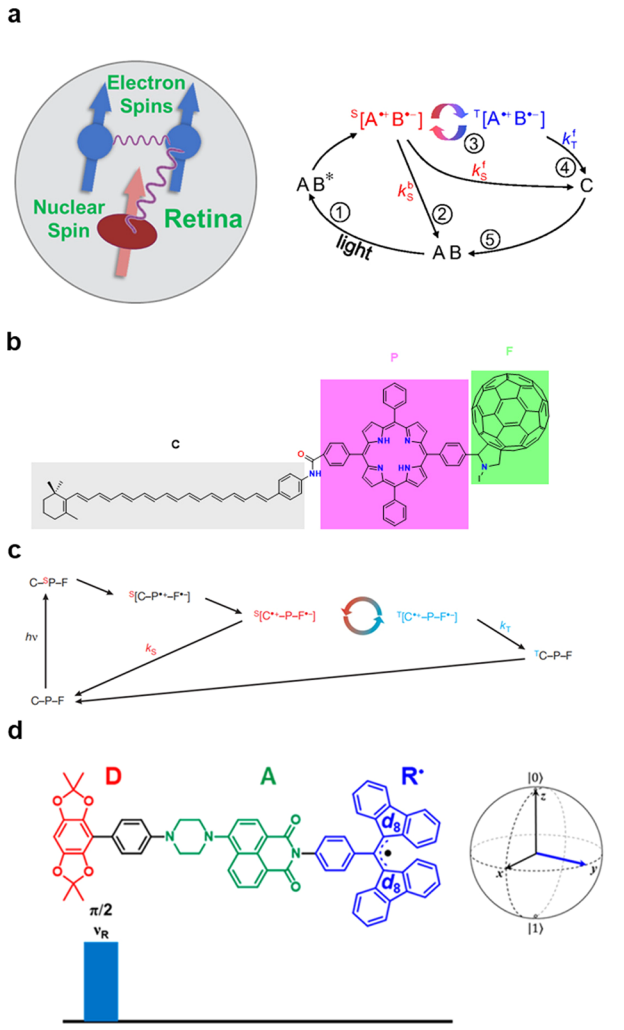

Figure 4. (a) Schematic of the radical-pair mechanism for magnetoreception.[97,151] Adapted with permission from ref 151. Copyright 2009 The National Academy of Sciences of the USA. (b and c) Reaction scheme of C−P−F triad to demonstrate the principle of a chemical compass[157] and (d) spin-entangled radical pairs in covalent D−A−R systems to demonstrate electron spin-state quantum teleportation.[171]

compass, called a "chemical compass", consisting of a triad linked carotenoid (C), porphyrin (P), and fullerene (F) groups has been reported (Figure 4b,c).[157] The singlet state radical pair (or biradical) $^{S}[C^{\bullet+}-P-F^{\bullet-}]$ can be produced efficiently by green light. After sequential reverse energy transfer, the radical can return to the ground state or be excited to triplet state $^{T}C-P-F$ and converted to radical pair $^{T}[C^{\bullet+}-P-F^{\bullet-}]$. The last process is sensitive to the magnetic field and is controlled by the magnetic interactions of two single electrons. Like other triads,[158,159] the lifetime of $[C^{\bullet+}-P-F^{\bullet-}]$ was tuned by applying a surrounding magnetic field. The relation between transient absorption of $[C^{\bullet+}-P-F^{\bullet-}]$ at 119 K and biphasic magnetic field indicates the expected magnetic field response of the radical pair.[160] The signal changes in transient absorption spectra below 1 mT was the "low field effect", indicating the product yields of radical reaction in solution.[123] The transient absorption of the radical pair was opposite at 100 and 400 ns with an applied external magnetic field, consistent with the expectations of the biphasic time dependence. More significantly, the absorbance changes in the radical pair can be up to ∼1.5% when performed in magnetic fields equivalent to that of the Earth, which seems to be the first observation of the chemical effect of a weak magnetic field of ∼50 μT.

$[C^{\bullet+}-P-F^{\bullet-}]$ can act as a chemical compass inspired by a magnetoreceptor *in vivo* with some distinguished properties—rapid response of absorption and long enough lifetime to be detected. Moreover, the radical centers are sufficiently separated, minimizing the inter-radical exchange and dipolar interactions which could interfere with the detection of the magnetic field.[160] Another attractive feature of $[C^{\bullet+}-P-F^{\bullet-}]$ is the highly asymmetric distribution of its magnetic nuclei, which is related to the optimal isotropic and anisotropic magnetic field effects.[161] Additionally, the results of transient absorption photoselection experiments show that the transition dipole moment of $C^{\bullet+}$ is primarily parallel to the long axis of C−P−F.[162] The results of these triad experiments, namely, the high sensitivity, may inform the future design of biologically inspired artificial chemical compass systems.

Although the feasibility of a chemical compass has been shown in the model systems,[162−164] the uncertainty remains given such anisotropic effects of natural magnetosensors under ambient conditions. In principle, a radical pair formed in a specific photoreceptor such as cryptochrome[144,165] is sensitive to the weak magnetic field such as the earth's magnetic field. Efficient sequential electron transfer along the radical chain can produce a well-separated (≥2 nm) radical pair with weak interaction between radicals and little back electron transfer (≥10 μs).[30]

One of the most promising avian magnetosensor systems is the flavin/tryptophan radical pair generated by blue light excitation in the protein cryptochrome.[151,166] However, the field effects *in vitro*, even applied with a relatively strong magnetic field, were limited in isolated proteins in isotropic solutions.[167]

Another possible chemical compass is the ascorbyl radical formed by the photoreaction between flavin and ascorbic acid.[168] In solution, the flavin/ascorbyl pair exhibited notable sensitivity to weak fields compared to previously reported systems. However, recent simulations via molecular dynamics point out that encounters of the ascorbyl radical with cryptochrome are too brief and infrequent to detect the earth field. These results imply that both experimental and theoretical studies are warranted to understand further the role of the radical hypothesis in synthetic systems of the chemical compass.

In addition, other donor−acceptor−radical (D−A−R) molecules with ultrafast photochemical electron transfer can produce a radical pair ($D^{\bullet+}-A^{\bullet-}$) leading to entangled two-spin singlet or triplet states (Figure 4d).[12,169−171] In an organic $D-A-R^{\bullet}$ molecule, a more stable radical $D^{\bullet+}$ instead of $R^{\bullet}$ will be formed, by which electron spin-state teleportation can be achieved to preserve quantum information over long distance.[172,173] After a spin state is prepared on $R^{\bullet}$ via a resonant microwave pulse, the singlet entangled electron spin pair $D^{\bullet+}-A^{\bullet-}$ is formed by the photoexcitation of A. Meanwhile, the Bell state measurement occurs when the radical pair $D^{\bullet+}-A^{\bullet-}-R^{\bullet}$ is converted to $D^{\bullet+}-A-R^{-}$ by a spontaneous ultrafast chemical reaction to achieve spin state teleportation, which can be confirmed by EPR spectroscopy. Experiments also showed excited-state spin wave functions of tripartite systems consisting of a stable organic radical covalently attached to a photogenerated electron−hole pair.[174] However, although some specific molecular quantum

https://doi.org/10.1021/acs.jpclett.4c00264
J. Phys. Chem. Lett. 2024, 15, 3294−3316

states can be achieved, these pure states are difficult to preserve due to vibronic coupling, making the addressing and reading of the quantum state very challenging.

Several factors could be considered in order to stabilize the charge transfer state in D−A−R systems. First, the electronic coupling between the D and A units can enhance charge transfer efficiency.[175] The energy levels of D and A should be well-designed. Second, steric hindrance[176] or electronic perturbations[177] can be introduced to accelerate the charge transfer process. Third, covalent interactions can be replaced by supramolecular interaction to prevent charge recombination and extend the lifetime of the charge transfer state.[178]

Despite the advances discussed above, future research on radical pair magnetoreceptors should focus more on high sensitivity against weak-field compass responses in oriented proteins. Furthermore, it is vital to identify the radical pair partners with optical or magnetic resonances via their spectral fingerprints. These studies should not be limited to the isolated proteins *in vitro*, but also focus on their performance *in vivo* so that the partners and solution conditions match where the proteins are found.[97]

Quantum sensors, based on properties such as coherence and entanglement, have the potential to increase sensitivity over their classical counterparts. However, there are many challenges to finding new material-based systems for quantum sensing. Radical spin systems are intriguing possibilities for quantum sensors, although they tend to suffer from short coherence times. We also turn to biology, such as avian magnetoreception, for inspiration in the design of future quantum sensing systems. In addition to looking at materials-based systems with molecular-scale quantum effects for quantum sensing, in the following sections, we also study materials that have unique quantum properties due to nonclassical intermolecular interactions.

Primitive marine algae and bacteria are remarkable for their ability to capture solar light and convert it to energy through photosynthesis.[58,179−187] The antennae-like systems are critical in the light-harvesting (LH) process because they can absorb light and transfer the excitation energy to the reaction center efficiently, with near-quantum unity.[58,181,188−190] Although the interaction between chromophores involved in light harvesting is generally weak, the chromophores can, in some instances, interact strongly to produce collective excitations called Frenkel excitons[81] that are delocalized over many molecules.[191]

J-aggregates are a class of organic molecular materials that exhibit narrow, red-shifted absorption bands with respect to the relevant monomer bands due to $\pi-\pi$ cofacial stacking of the molecules.[78] The transition dipoles of *J*-aggregates are arranged in a head-to-tail fashion, and the dipoles that oscillate in-phase lower the energy of the excitonic state in comparison to that of the monomer, which explains the bathochromic shift in absorption band and the small Stokes shift in fluorescence spectra.[192] The subtle features of *J*-aggregates cannot be well explained by the conventional theory of exciton dynamics. Some entanglement entities such as von Neumann entropy, Wooters concurrence, the Meyer-Wallach measure, and the quantum discord proved the quantum information attributes of *J*-aggregates.[193]

The very first *J*-aggregates reported were formed in aqueous solution of pseudoisocyanine chloride (1,1′-diethyl-2,2′-cyanine chloride; PIC), in which the chromophores self-assembled and were stacked like a polymer.[78] Since then, the *J*-aggregates of cyanine dyes have been studied extensively. One recent example is the *J*-aggregate-forming dye 5,6-dichloro-2-[[5,6-dichloro-1-ethyl-3-(4-sulfobutyl)benzimidazol-2-ylidene]propenyl]-1-ethyl-3-(4-sulfobutyl)benzimidazolium hydroxide, sodium salt, inner salt (TDBC).[194] It is a highly delocalized π-electron system that shows exceptionally narrow absorption and photoluminescence line width, and this property is utilized to study the effect of Raman-mediated polariton scattering.[195] It was concluded that the collective vibration of a large number of molecules leads to an enhancement in the intensity of certain Raman-active modes, namely, the aggregation-enhanced Raman scattering (AERS).[194] This result provides researchers insight into how molecular vibrations play a role in electronic coupling of molecules in *J*-aggregates, which is important for the development of polariton-based devices, microcavity LEDs, and hybrid organic−inorganic optoelectronic devices.[194]

H-aggregates are organic molecular aggregates with an absorption band showing a hypsochromic shift and suppressed radiative decay rate in comparison to the relevant monomer.[196] Their transition dipoles are aligned side-by-side, and the excitonic state that has the highest transition probability based on Fermi's golden rule is higher in energy than that of the monomer, which induces the spectral blue-shift.[81,192] A representative example of an H-type aggregate is the perylene tetracarboxylic acid bisimide (PBI) oligomer aggregates, which is a $\pi-\pi$ stacked helical self-assembly.[197] In these extended PBI aggregates, long-range coherent energy transfer was found to precede excimer formation, and this understanding is important in future studies of molecular aggregates to fabricate higher performance optoelectronic materials.[81]

In nature, Frenkel excitons are the electronic states of the natural bacteriochlorophylls (BChls) c, d, e in the chlorosomes of green bacteria.[78] They comprise an efficient light-harvesting system that absorbs light in the near-IR spectral region.[78,198] The supramolecular motif of the slip-stacked *J*-aggregates in light-harvesting antenna complex exhibits excellent optical properties such as efficient exciton coupling and fast exciton energy migration, which inspires the design of synthetic light-harvesting devices and artificial supramolecular assemblies.[199]

In the following discussion, we first introduce biological systems with a focus on intermolecular interactions. We then discuss nature-inspired supramolecular systems with similar intermolecular interactions and possibly quantum properties.

Before the twentieth century, biological systems seemed to be too sophisticated to be explained with mathematical or chemical methods. However, enormous progress has spurred much interest in exploring whether quantum mechanics plays a role in biological systems. Although every chemical process involves quantum mechanics,[200] in many ways quantum mechanics was still a concept alien to biology.[97] But with the advances in many microscopies and spectroscopies, scientists began to unearth relationships between physics and microscopic biological systems.[201] Different from applications in quantum information, nonclassical phenomena in biology can be subtle. Despite some criticism,[202,203] researchers remain optimistic that nontrivial quantum effects might play a role in some biological functions.

LH centers in photosynthetic species can absorb photons from the sun as electronic excitation, which are then transported to a reaction center (RC) where charge separation creates stable chemical energy. However, the precise structures and pigments in the LH center differ in different organisms.[204]

https://doi.org/10.1021/acs.jpclett.4c00264
J. Phys. Chem. Lett. 2024, 15, 3294−3316

In this section, we discuss the architecture and nonclassical effects arising from intermolecular interactions in light-harvesting systems.

The observation of quantum coherent dynamics in a light-harvesting system was first observed by Engel and colleagues[179] in the Fenna−Matthews−Olson (FMO) complex of green sulfur bacteria. Within this photosynthetic bacterium, energy is transferred to the RC through the FMO complex, which has a trimeric structure with each monomer composed of eight bachteriochlorophyll *a* (BChl-*a*) pigments (Figure 5a).[205] Researchers proposed the spectroscopic observation of quantum coherence of an electronic excitation inside the FMO complex at 77 K using 2DES.[179] Further research on mutant FMO complexes showed that coherent oscillations are largely insensitive to altering the exciton and that interchromophore couplings between BChls are vibronic in nature on the excited state and lead to delocalization of excitonic states.[206] Room-temperature coherent oscillations and the assigned vibronic modes for the wild type FMO complex are shown in Figure 5b,c. While the current consensus is that quantum coherence is not a prominent effect in the FMO complex, the energy transfer mechanism is certainly not simply incoherent hopping (like Förster theory assumes), and therefore, the FMO complex has become an important model system for benchmarking quantum dynamics methods.

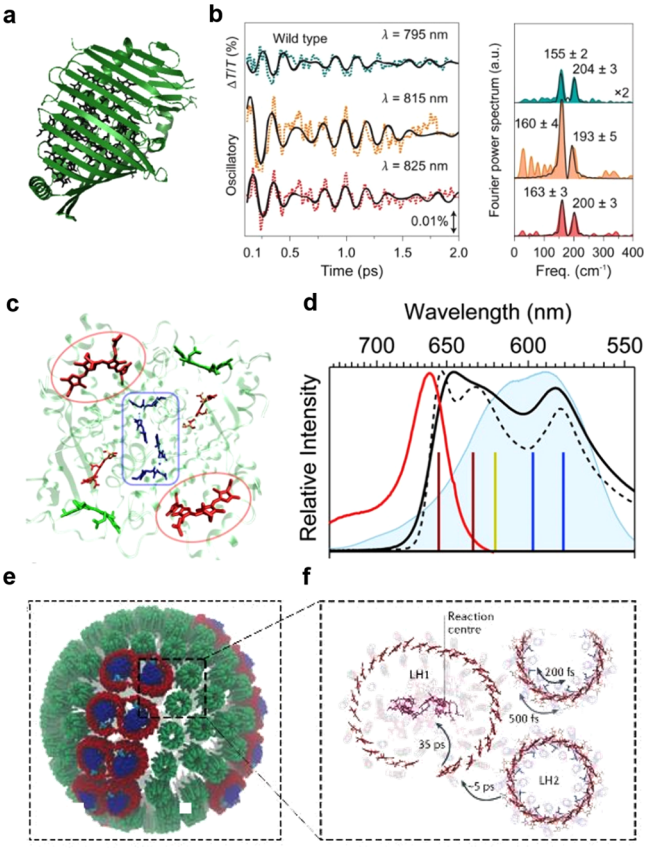

Figure 5. Photosynthetic systems. (a) Crystal structure of the Fenna−Matthews−Olson Protein from *Chlorobaculum tepidum* (3ENI).[206] (b) Measured coherent oscillations at room temperature (left) and Fourier power spectra with assigned vibronic modes (right).[206] (c) Crystal structure of Phycocyanin 645 from *Chroomonas mesostigmatica* (4LMS) with color-coded bilins: dihydrobiliverdin (blue), mesobiliverdin (green), and phycocyanobilin (red).[215] (d) Color-coded stick spectra show the absorbance of the bilins overlaid with the laser spectrum (shaded blue), room-temperature absorbance (solid black), and fluorescence (red) curves.[215] (e) Schematic illustration of supramolecular architecture of the photosynthetic chromatophore vesicle in purple bacteria.[75] (f) Molecular structure of the LH1 and LH2 units with associated exciton-transfer time scale within and between the two proteins of *Rhodospirillum photometricum*.[98]

These studies of the FMO complex inspired investigations of other photosynthetic systems with supramolecular assemblies of chromophores, including light-harvesting complex 2 (LH2) from purple bacteria and phycobiliproteins in algae and cyanobacteria.

The light-harvesting antenna proteins of cryptophyte algae, complexes called phycobiliproteins (PBPs), are interesting LH systems to study because of their unique photophysical properties.[207−213] The PBPs will have either an open conformation, where there is a water-filled gap in the center of the structure, or a closed conformation, where there is no gap and the central chromophores are in close proximity.[214] The difference in conformation is linked to differences in excitation energy transfer (EET) efficiency; it has been observed that EET in PBPs with closed conformations occurs approximately twice as fast as their open counterparts.[210] It is proposed that the central dimer in closed-form PBPs, such as phycocyanin 645 (PC645) and phycoerythrin 545 (PE545), form a molecular excitonic dimer due to strong coupling.[180] Figure 5c,d shows the main chromophores in PC645, along with their relative contributions to the absorbance spectrum. The dihydrobiliverdins (DBVs) are strongly coupled to form a molecular exciton dimer and serve as the donor, while the phycocyanobilins (PCBs) are the terminal acceptors.[180,215] As a result, excitation is delocalized and the lower exciton state of the donor is in closer resonance with the acceptor $n = 1$ excited state, facilitating EET. These intermolecular nonclassical effects have been observed via broadband transient absorption spectroscopy,[210] two-dimensional photon echo,[180] two-dimensional electronic spectroscopy (2DES),[215] and two-dimensional electronic vibrational spectroscopy,[216] and there is a proposed vibronic coupling mechanism for energy transfer in PC645.[215] The delocalization across donor chromophores, vibronic coupling mechanism, and related rapid EET rates for closed conformation PBPs demonstrate that intermolecular interactions within LH systems, even at the simple dimer level, make the ultrafast dynamics of light harvesting nontrivial.

In addition to cryptophyte algae, phycobiliproteins are also found within the light-harvesting peripheral proteins of red algae and cyanobacteria.[217,218] These LH systems are called phycobilisomes, and they contain a series of PBPs as the cylindrical rods arranged in trimers or hexamers attached to a core.[219] This scaffold of PBPs forms an energy funnel; phycoerythrin and C-phycocyanin make up the rods of the phycobilisome, and allophycocyanin makes up the core and serves as the terminal emitter.[220] A 2DES study of cyanobacterium *Fremyella diplosiphon* phycobilisome showed that, under broadband excitation, delocalization of excitations in the bilins of the phycobilisome rods aid energy transfer down the rod with a subpicosecond time scale before localization occurs.[221]

Prominent delocalized excitation is observed in the antenna complexes of purple bacteria. The light-harvesting center in purple bacteria is formed as a cellular membrane, which consists of hundreds of spherical bulbs of 60 nm in diameter and/or lamellar sheets. Figure 5e shows the LH center found

https://doi.org/10.1021/acs.jpclett.4c00264
J. Phys. Chem. Lett. 2024, 15, 3294−3316

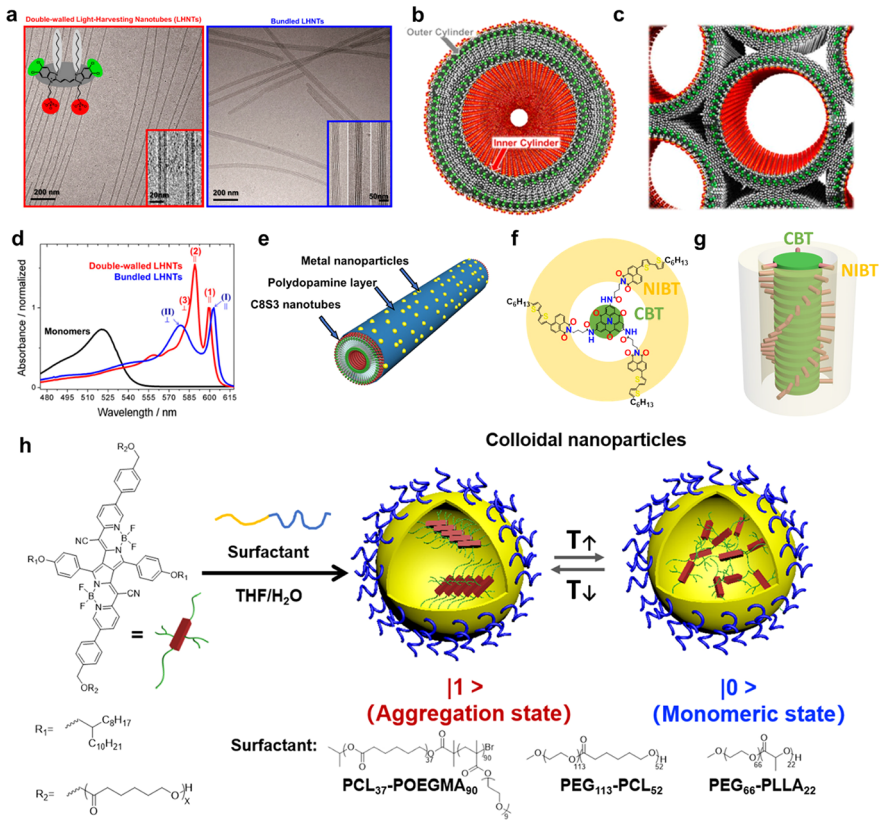

Figure 6. Bioinspired quantum materials and technologies. (a) Cryo-EM image of double-walled LHNTs (red) and bundled LHNTs (blue) self-assembled by C8S3.[238] (b) Schematic diagram of LHNTs consisting of two concentric cylinders self-assembled by C8S3.[238] (c) Schematic diagram of bundled LHNTs.[238] (d) Absorption spectra of C8S3 dye in monomer in methanol (black); double-walled LHNTs in water/methanol (red) and bundles of LHNTs (blue).[238] Adapted with permission from ref 238. Copyright 2014 The National Academy of Sciences of the USA. (e) Schematic presentation of DPA stabilized LHNTs functionalized with metal NPs.[245] (f) Chemical structure and (g) schematic illustration of CBT-NIBTs nanofibers.[251] (h) Schematic presentation of chemical structure of pyrrolopyrrole cyanine (PPCy) chromophore as molecular qubits, the preparation of colloidal nanoparticles in the presence of an amphiphilic block copolymer as surfactant, and temperature-induced reversible transformation between J-aggregation state ("1") at a low temperature and monomeric state ("0") at a high temperature. (x represents the number-average degree of polymerization.)[254]

in *Rhodobacter (Rba.) spheroids*,[222,223] composed of three proteins, RC (blue), light-harvesting complexes 1 (LH1, red), and light-harvesting complexes 2 (LH2, green). The sphere is formed by a lipid bilayer consisting of over 200 transmembrane proteins, which are composed of 1000 carotenoids and 3000 bacteriochlorophylls (BChls). In each arrangement unit, 56 BChls form an S-shaped line in a dimer of LH1 and 18 BChls and 9 BChls form a ring and a crown, respectively, in each LH2. The RC, composed of four BChls, two bacteriopheophytins, an iron atom, and a permanently and a temporarily bound quinone, is fitted in a ring-like protein of LH1.[223] Although all BChls in RC are involved in light absorption, only two BChls lying close to a 2-fold symmetry axis are the main acceptor of light excitation, and the two BChls form a so-called "special pair". The special pair uses 2-fold symmetry to enhance RC absorption ability and electronic coupling to LH1 BChls through superradiance,[224] which involves a quantum coherence effect to speed up excitation transfer[225] between RC BChls and LH1 BChls.

In the LH apparatus, the BChls in RC are the final reception of light energy, which can directly absorb light energy or receive excitation energy transferred from LH1 BChls, while BChls in LH1 can also absorb sunlight directly or accumulate excitation energy from nearby LH1 BChls or LH2 BChls. As the main light energy source, the number of LH2 BChls is more than four times that of the RC and LH1 BChls. Delocalization of the excited states of BChls in LH1 and LH2 is important for light harvesting.[74,225]

The structures of LH2 and LH1 are shown in Figure 5f. In LH2, there are two concentric rings called B800 and B850 rings which have absorption at 800 and 850 nm, respectively, while LH1 has a B875 with red-shifted absorption.[189] The self-assembly process of LH complexes of bacterial photosynthetic systems consists of two tiers. In the first tier, two bacteriochlorophyll α (BChl α) associate with one α-peptide and one β-peptide to give an $\alpha\beta$-subunit or with two β-peptides to give $\beta\beta$-subunits.[226,227] In the second tier, the $\alpha\beta$-subunits associate with each other to give cyclic oligomers.[228] As observed in bacterial species, the number of $\alpha\beta$-subunits in the LH2 rings is usually 8 or 9.[228,229] It is worth noting that the assembly processes result in spectral changes owing to the interaction of BChl α with each other or proteins.[227] The monomeric BChl α in toluene has an absorption at ~780 nm, while the absorption of an $\alpha\beta$-subunit or $\beta\beta$-subunit red-shifts to ~820 nm. Further, the absorption of cyclic oligomers in LH2 shifts to ~850 nm when the number of interacting BChl α molecules increases to 16 or 18. The delocalization length in the B850 circular aggregate of LH2 was found to be across 4 BChls.[230] Exciton−exciton annihilation experiments have

https://doi.org/10.1021/acs.jpclett.4c00264
J. Phys. Chem. Lett. 2024, 15, 3294−3316

measured exciton diffusion within a few picoseconds in purple bacteria membranes.[189]

Due to the lower excitation energy of LH1, energy transfer from LH2 to LH1 is favored, followed by funneling of the excitation energy into the RC. In LH1 complexes, the cyclic architectures and the number of interacting BChl α are further increased to 32, resulting in an additional bathochromic shift to ∼875 nm. Through biological evolution, the photosynthetic systems pack a maximal number of BChls into the available membrane, with room for critical chemical reactions in a self-organized process. Meanwhile, the system is stable enough against unavoidable damage to its components due to its structural simplicity.[189] These results provided much insight for the study of the structure−function relationships in both natural and synthetic systems.

Nature assembles molecular chromophores into supramolecular structures, which are further assembled into close-packed superstructures to improve the efficiency of LH systems.[58,181,184,188,191] Such hierarchical assembly of chlorophyll dyes in the natural LH system shows optical characteristics of typical *J*-aggregation. To mimic the structure and function of light-harvesting systems in photosynthesis, research efforts have been devoted to a series of synthetic chromophores that can self-assemble into ordered structures in the micro/nanoscale.[86,188,231−233]

Inspired by the green sulfur bacteria, which can harvest light with high efficiency, a closely packed assembly of several amphiphilic chromophores into *J*-aggregation artificial LH supramolecular complexes is required to maximize the light-absorption ability. Figure 6a shows a cryo-electron microscopy (cryo-EM) image of light-harvesting nanotubes (LHNTs) consisting of an amphiphilic cyanine dye, 3,3′-bis(2-sulphopropyl)-5,5′,6,6′-tetrachloro-1,1′-dioctylbenzimideacarbocyanine (C8S3), which self-assembles into a uniform supramolecular structure composed of two concentric cylinders, as schematically illustrated in Figure 6b with an inner cylinder of a diameter of ∼6 nm and outer cylinder of a diameter of ∼13 nm.[234] These double-walled LHNTs mimic the circular aggregate structure found in the light-harvesting architecture of purple bacteria, whose properties are discussed in a previous section.

Upon the formation of LHNTs, the broad absorption band of the monomer disappeared, accompanied by the emergence of two prominent absorption peaks that are narrow and red-shifted, indicating the strong excitation transfer between molecular transition dipole moments (Figure 6d).[235] Redox chemistry and flash dilution experiments show that peaks (1) and (3) at 599 and 580 nm correspond to the inner layer of the double-walled LHNTs, while peak (2) at 589 nm corresponds to the outer layer.[235] The band (1) with low-energy and narrow peaks indicates large exciton delocalization.[236,237] Moreover, the outer layer of double-walled LHNTs can be eliminated through redox chemistry or flash dilution, indicating that the two cylindrical systems are weakly coupled and can be effectively decoupled since the absorption spectrum shows that the two layers of LHNTs are independent.[235,238] The absorption spectrum of C8S3 LHNTs systems can be simplified as the sum of the individual spectra of two cylindrical aggregates, which is further evidence of a weakly coupled system.[19]

More interestingly, the double-walled LHNTs, upon aging in an aqueous solution, further self-assemble into bundled LHNTs (Figure 6c), which can be detected by absorption spectroscopy.[238] After bundling, the two main absorption peaks of double-walled LHNTs at 599 (band 1) and 589 nm (band 2) are transformed into two new absorption peaks at 603 (band I) and 575 nm (band II), respectively (Figure 6d). For double-walled LHNTs, bands 1 and 2 are polarized primarily parallel to the cylindrical axis and band 3 is polarized primarily perpendicular to it. For bundled LHNTs, band I and band II are primarily polarized perpendicular to each other.[238]

To unravel the energy transport in LHNTs, a spectroscopic lab-on-a-chip approach was employed, in which ultrafast coherent dimensional spectroscopy and microfluidics were working in tandem with theoretical modeling.[239] At low excitation fluences, the outer layer acts as an exciton antenna, supplying excitons to the inner tube. However, at high excitation fluences, the outer layer depletes the exciton population before any exciton transfer. To investigate the exciton migration, the LHNTs were stabilized in a sucrose glass matrix to reduce light and oxidation.[240] The exciton diffusion lengths and constants were estimated with exciton−exciton annihilation (EEA). By probing the signal of EEA compared with ultrafast and continuous wave laser excitations, both photoluminescence lifetimes and relative quantum yields are strongly mitigated and fit to a one-dimensional diffusion model to estimate exciton transport. The average exciton diffusion constant of LHNTs is 55 ± 20 cm^2/s, which is notably high for organic systems reported to date.[240]

However, the pristine C8S3 LHNTs are intrinsically dynamic and not stable against environmental changes, such as dilution, light irradiation, and heating. Several strategies have been reported to stabilize the LHNTs with polyelectrolytes,[241] silica shells,[242−244] or sucrose glass matrix.[240] Nevertheless, the coating of polyelectrolytes or silica shells lacks uniformity, and the dispersion into the glassy matrix of sucrose lacks further chemical addressability of the LHNTs. More recently, Wang's group proposed a mussel-inspired coating method to both stabilize and functionalize C8S3 NTs (Figure 6e).[245] By *in situ* polymerization on the surface of C8S3 LHNTs, a thin layer of polydopamine (PDA) formed on the surfaces of the C8S3 NTs. After PDA-coating, the thermal stability, photostability, and dynamic stability have been improved significantly. The PDA-coated NTs can be further functionalized with other inorganic materials, such as metal ions or metal nanoparticles, to prepare multifunctional nanocomposites that could supply interesting model systems for the study of photosynthesis.

This *J*-aggregate supramolecular circular aggregate shows that intermolecular interactions lead to delocalized excitation, similar to circular aggregates found in nature, such as the B850 ring of LH2. The LHNT is an example of a synthetically available bioinspired system with nonclassical properties due to intermolecular interactions within the supramolecular assembly.

Similarly, some attention has been paid to *H*-aggregation nanofibers with more efficient long-range energy transportation along the supramolecular architectures.[246−248] In a recent study,[246] stable and robust supramolecular structures of carbonyl-bridged triarylamine trisamide (CBT) linked with 4-(5-hexyl-2,2′-bithiophene)-naphthalimides (NIBTs) can be formed in different solvents (Figure 6f,g). CBT can self-assemble into single supramolecular nanofibers in *n*-dodecane and bundles of supramolecular nanofibers in anisole. Absorption spectroscopy shows that supramolecular nanofibers have a lower energy peak than CBT monomers, while single

https://doi.org/10.1021/acs.jpclett.4c00264
J. Phys. Chem. Lett. 2024, 15, 3294−3316

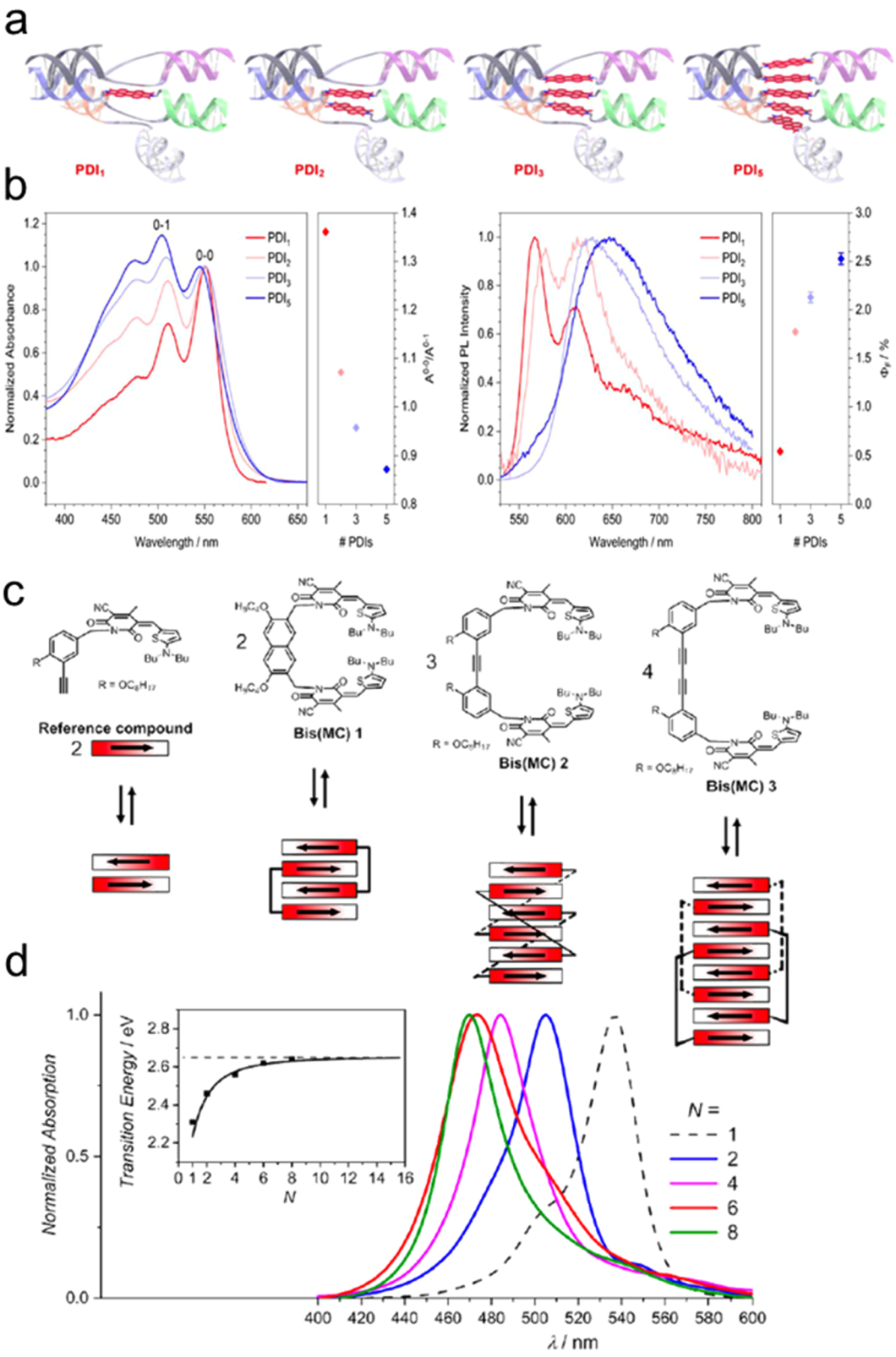

Figure 7. (a) Schematic representation of assembling organic semiconductors via DNA scaffolds.[233] (b) Left: Absorption spectra of PDI_1−PDI_5; Right: Photoluminescence (PL) emission spectra and quantum yields (Φ_F) of the PDI/DNA constructs.[233] Adapted with permission from ref 233. Copyright 2022 American Chemical Society. (c) Chemical structures and schematic representation of the self-assembly process of MC dyes.[261] (d) UV/vis absorption spectra of monomer and dimeric stack of MC, tetrachromophoric stack of Bis(MC) 1, hexachromophoric stack of Bis(MC) 2, and octachromophoric stack of Bis(MC) 3 in THF/MCH mixture (17.5:82.5) (insert: Fit of the peak positions corresponding to the highest exciton state of the respective aggregates as a function of the number of stacked chromophores N).[261] Adapted with permission from ref 261. Copyright 2019 American Chemical Society.

https://doi.org/10.1021/acs.jpclett.4c00264
J. Phys. Chem. Lett. 2024, 15, 3294−3316

supramolecular nanofibers have lower energy than bundled ones, which is characteristic of delocalized excitons in *H*-aggregates.[81] Photoluminescence decay curves show the exciton movement in nanofibers in which the initial singlet exciton population, created by the diffraction-limited excitation pulse, is transported away from the excitation spot before (radiative) decay, which is more pronounced for the single nanofiber than the bundle of nanofibers.[246]

The photoluminescence spectra from diluted nanofibers (0.07 μM) indicated that peripheral NIBT units had no influence on exciton transport over macroscopic distances.[249,250] The long-range exciton transfer was enabled by electronic coupling and occurred along the ordered nanofiber core, which produced vibronic singlet excitons with the lowest-energy transition having a small transition dipole moment.[251] The irreversible energy transfer to the NIBT periphery leads to the loss of electronic excitations from CBT units.[252] Nevertheless, the exciton energy can be trapped at defects in the CBT cores, where the PL reaches its maximum because of the small defects within the fiber core. Thus, the weak PL signal from the CBT core indicates the highly ordered structure of the nanofiber.

The *H*-aggregation nanofibers with such a long excitation transport range bring inspiration to the development of new quantum materials. On the one hand, such *H*-aggregation nanofibers can be applied to transport energy from LH systems to transducers to convert it into charge carriers more efficiently. On the other hand, the strongly reduced transition dipole moment in *H*-aggregation nanofibers is beneficial to achieving stable charge-separated states.[251]

These experimental results add a new dimension to the development of a detailed theoretical understanding of energy transport in both *J*-type and columnar *H*-type supramolecular nanostructures.[253] Both *J*- and *H*-type supramolecular structures are useful for energy transport in an efficient and directed way from an LH antenna system to a transducer for conversion into charge carriers. In contrast, *H*-type nanostructures exhibit a longer transport range than *J*-type ones because of the strong electronic coupling between units in *H*-aggregates.[246] However, compared with natural LH systems, the energy transport efficiency and stability of synthetic systems are far from enough. Further efforts should be devoted to stabilizing synthetic LH systems and improving the energy transport efficiency.

Recently, Wang's group presented a new type of supramolecular qubits and nanoparticle ensembles based on the thermally controllable transformation between *J*-aggregation and monomeric states of molecular chromophores, using pyrrolopyrrole cyanine (PPcy) tethered with polymeric chains such as polycaprolactones as an example (Figure 6h).[254] Colloidal nanoparticles (NPs) composed of the polymer-tethered PPcy chromophores showed a red-shifted, narrow absorption peak and PL emission at low temperatures (e.g., 25 °C), in contrast to the broad absorption peak and PL emission of the monomeric state of the chromophores at a high temperature (e.g., 70 °C). The thermal transformation between *J*-aggregation and monomeric states is highly controllable and reversible within tens of cycles. Moreover, we studied the effect of chemical composition and chain length of polyesters on aggregation and optical properties.[231] The *J*-aggregation, *H*-aggregation, and monomeric states are tuned by variations of the polymer chain lengths and compositions.[231] Such supramolecular quantum systems, resembling some features of LH complexes in photosynthesis, might provide new opportunities for processing quantum information under mild conditions, which do not require complicated ultracooling and/or high vacuum systems.

Some theoretical research has been carried out, for example, by Thilagam, to explore the implication of *J*-aggregates of organic chromophores relevant to quantum computation and quantum information processing.[255] Photon absorption can be applied to initiate *J*-aggregate from the monomeric state ($|0\rangle$) to the excited state ($|1\rangle$), like the Hadamard gate. The electronic excitation can propagate to *N* molecular sites with unique wavevector and energy levels and give rise to the superposition of several such states. The main errors originate from annihilation or relaxation processes during exciton transfer. In addition, it has been conjectured that some quantum algorithms such as Grover-like search can be realized by quantum *J*-aggregate systems.[256] However, the genuine multipartite entanglement of the *J*-aggregate still requires experimental proof.

Recently, the aggregation number of perylene diimide (PDI) has been reported to be precisely controlled by well-defined semiconductor/DNA constructs (Figure 7a).[233] The PDIs are integrated within DNA chains using phosphoramidite coupling chemistry, allowing the selection of the DNA sequence to either side and the specification of intermolecular DNA hybridization. By choosing different DNA, PDI_{1-5} can be achieved. The steric hindrance and charge of the surrounding DNA eliminate interactions with neighboring constructs. Consequently, the DNA-based assemblies represent an isolated and well-defined quantum system.

The optical properties of PDI are sensitive to the aggregation state in a unique way (Figure 7b left). The absorption peaks at ∼510 and ∼550 nm correspond to the 0−0 (A^{0-0}) and 0−1 vibronic bands (A^{0-1}), respectively. The coupling between two PDI molecules can reduce the vibronic peak ratio (A^{0-0}/A^{0-1}) from >1.3 to <0.9. The decreased vibronic peak ratio (A_{0-0}/A_{0-1}) indicated stronger *H*-coupling between the PDI constructs. The photoluminescence (PL) emission spectra (Figure 7b right) further confirm the relationship between aggregation and optical properties of PDI constructs that with increasing *H*-aggregation of PDIs, the steady-state emission red-shifted and became broader. However, the PL quantum efficiency (Φ_F) increased with the number of PDIs due to suppressed competing relaxation pathways, which contradicted the optical properties of the classic *H*-aggregates.

Würthner and co-workers reported another example of organic dye formed by the linkage of bis(merocyanine) (Bis(MC)) dyes with spacer moieties of different lengths, which direct formation of well-defined aggregates from dimer up to octamer (Figure 7c).[232] After Bis(MC) was synthesized with different spaces between chromophores (from 7.3 to 9.5 to 10.9 Å), the self-assembly of Bis(MC) can be controlled by a new concept of spacer-encoded self-assembly. Their self-assembly into tri- and tetramolecular systems was analyzed by UV/vis spectroscopy (Figure 7d). The increase in aggregation size leads to a blue shift of the absorption peak corresponding to the highest exciton state. These results are consistent with the calculation results by time-dependent density functional theory.

By precisely controlling the intermolecular distance between donor−acceptor (D−A) molecules on surfaces of solid substrates, Hou and co-workers recently reported an

https://doi.org/10.1021/acs.jpclett.4c00264
J. Phys. Chem. Lett. 2024, 15, 3294−3316

incoherent-to-coherent transition in intermolecular electronic energy transfer (EET).[257] The intermolecular EET from a donor (platinum phthalocyanine (PtPc)) to an acceptor (zinc phthalocyanine (ZnPc)) was selected because of its rich optoelectronic properties and structural similarities. The molecules were first decoupled by a three-monolayer NaCl spacer from the Ag(100) substrate underneath. The scanning-tunneling microscopy-induced luminescence (STML) spectrum of isolated D−A molecules showed two sharp and separate emission peaks at 637.7 and 652.3 nm, corresponding to PtPc and ZnPc, respectively, which could be attributed to the intrinsic Q(0,0) transition of the neutral molecular states. Then, when pushing isolated ZnPc toward PtPc to a distance of ∼2.21 nm, both characteristic emissions of PtPc and ZnPc can be detected by STML from PtPc, demonstrating the initiation of intermolecular EET from excited PtPc to ZnPc. Furthermore, when the intermolecular distance was less than 1.72 nm, the abrupt drop in the emission of ZnPc reflected the EET in a new regime. Two emerging peaks showed a blue-shift of the emission peak of PtPc to ∼636.6 nm, while a red-shift was shown to ∼657.5 nm for ZnPc. More importantly, the new peaks can be observed regardless of the position of the tips (either above ZnPc or PtPc) and the occurrence of coherent dipole coupling between PtPc and ZnPc in the heterodimer.[258] In other words, the excitation energy can transfer not only from the donor to the acceptor but also from the acceptor back to the donor. These results proved that the coherent channel was 3 times more efficient than a decoherent channel with the one-step process, offering compelling evidence for quantum coherence in D−A systems at the single-molecule level.

The ability to tune intermolecular distances between donor−acceptor systems and within supramolecular systems allows for synthetic control over steady-state properties as well as exciton dynamics. The collective effects observed in these systems result from intermolecular interactions, and the coherence of these states may be potential resources for quantum information technologies at ambient temperatures, although it remains challenging how to scale up the fabrication of ordered arrays of D−A molecules or supramolecular systems with controllable intermolecular distance and coupling relevant for QIT.

Quantum information science is a growing field of exploration with the search for better qubit materials with long coherence times and high sensitivity. With progress typically focused on atomic systems, here instead we explore progress in the search for materials-based qubits and molecular systems, exploiting intermolecular interactions that might serve as resources for nonclassical phenomena. Materials-based systems have the advantage of scalability and tunability via synthetic pathways, although they tend to suffer from short coherence times. We also noted how biology can serve as inspiration for quantum phenomena, exemplified by avian magnetoreception and, more subtlely, in photosynthetic light-harvesting systems.

For molecular systems, radical spin and nuclear spin exhibit extremely high controllability and scalability via chemical reactions. There are various experiments showing the feasibility of spin-based qubits. However, decoherence remains a problem for application. Although some techniques like embedding into MOFs, fullerenes, or mesoporous silica hosts mentioned above, shortcomings are still obvious: the synthesis yield is low, and the process is complex. Besides, the requirement of operation temperature is strict (a few or tens of K).

In biological systems, BChl assembles with different scales possessing variable optical properties, inspiring chemists to synthesize organic dyes with different aggregation sizes or intermolecular distances sharing similar properties. By elaborate molecular design, synthetic supramolecular dyes have more stability and tunability than do other systems. Such tunable optical properties are believed to be attributed to interaction at the nanometer level. However, the application of supramolecular systems in QIT is rarely reported.[259,260]

Chemical materials offer a vast diversity of structures on a hierarchy of length scales. Self-organization of molecular components can introduce strong or weak couplings between them that are useful for controlling electron transfer or excitation energy transfer or producing modestly delocalized molecular excitons. Owing to fast relaxation of higher, multiexcitation excited states, as well as a dearth of examples of very high spin states of chemical materials, it appears unlikely that these systems will be useful building blocks for qubits because we cannot generate the entire tensor product state space. Therefore, resources that will possibly be relevant for quantum information science based on chemical materials will likely be focused on properties of a truncated Hilbert space, for example, the single-excitation subspace. Thus, we imagine that the quantum properties hosted by chemical materials will have different applications and properties than precisely engineered systems being developed with quantum computation, etc., in mind. Those applications and properties have yet to be elucidated. Short-term questions include how weak quantum correlations are manifest in complex materials and how they scale with size and complexity.

AUTHOR INFORMATION

Corresponding Authors

Gregory D. Scholes − *Department of Chemistry, Princeton University, Princeton, New Jersey 08544, United States;* orcid.org/0000-0003-3336-7960; Email: gscholes@princeton.edu

Mingfeng Wang − *School of Science and Engineering, The Chinese University of Hong Kong, Shenzhen, Guangdong 518172, P. R. China;* orcid.org/0000-0002-6445-6854; Email: wangmingfeng@cuhk.edu.cn

Authors

Yipeng Zhang − *School of Science and Engineering, The Chinese University of Hong Kong, Shenzhen, Guangdong 518172, P. R. China*

Catrina P. Oberg − *Department of Chemistry, Princeton University, Princeton, New Jersey 08544, United States;* orcid.org/0000-0002-6935-9068

Yue Hu − *Department of Chemistry, Princeton University, Princeton, New Jersey 08544, United States*

Hongxue Xu − *School of Science and Engineering, The Chinese University of Hong Kong, Shenzhen, Guangdong 518172, P. R. China*

Mengwen Yan − *School of Science and Engineering, The Chinese University of Hong Kong, Shenzhen, Guangdong 518172, P. R. China*

Complete contact information is available at: https://pubs.acs.org/10.1021/acs.jpclett.4c00264

https://doi.org/10.1021/acs.jpclett.4c00264
J. Phys. Chem. Lett. 2024, 15, 3294−3316

Notes

The authors declare no competing financial interest.

■ ACKNOWLEDGMENTS

We acknowledge the financial support by the University Development Fund − Research Start-up Fund (UDF01001806) from the Chinese University of Hong Kong, Shenzhen. Y.Z. acknowledges the financial support of Ph.D. Scholarship from the Chinese University of Hong Kong, Shenzhen. C.O., Y.H., and G.D.S. acknowledge financial support from the National Science Foundation under Grant No. 2211326 and the Division of Chemical Sciences, Geosciences and Biosciences, Office of Basic Energy Sciences, of the US Department of Energy through Grant No. DE-SC0015429.

■ ABBREVIATIONS

Quantum information technology, QIT; Quantum dots, QDs; Photoluminescence, PL; Light-emitting diodes, LEDs; Light-harvesting, LH; Quantum charge-coupled device, QCCD; Quantum electrodynamics, QED; Electron paramagnetic resonance, EPR; Nuclear magnetic resonance, NMR; Santa Barbara Amorphous, SBA; Blatter-type bis(triethoxysilylvinyl)-triazinyl radical, BTEV-BTR; Thermogravimetric analysis, TGA; Continuous-wave, CW; Hyperfine interaction, HFI; Triphenylmethyl, TM; Phthalocyanine, Pc; Metal−organic frameworks, MOFs; Reaction center, RC; Special pair, SP; Fenna−Matthews−Olson, FMO; Cryo-electron microscopy, cryo-EM; 3,3′-bis(2-sulphopropyl)-5,5′,6,6′-tetrachloro-1,1′-dioctylbenzimideacarbocyanine, C8S3; Exciton−exciton annihilation, EEA; Polydopamine, PDA; Carbonyl-bridged triarylamine trisamide, CBT; 4-(5-hexyl-2,2′-bithiophene)-naphthalimides, NIBTs; Pyrrolopyrrole cyanine, PPcy; Nanoparticles, NPs; Perylene diimide, PDI; Electronic energy transfer, EET; Scanning tunneling microscopy-induced luminescence, STML

■ REFERENCES

(1) Nielson, M. A.; Chuang, I. L. *Quantum Computation and Quantum Information*; Cambridge University Press: Cambridge, 2000.
(2) DiVincenzo, D. P. The physical implementation of quantum computation. *Fortschritte der Phys.* **2000**, *48* (9−11), 771−783.
(3) Feynman, R. P. Simulating physics with computers. *Int. J. Theor. Phys.* **1982**, *21* (6-7), 467−488.
(4) Igeta, K.; Yamamoto, Y. Quantum mechanical computers with single atom and photon fields. In *International Quantum Electronics Conference*, 1988.
(5) Zhong, H.-S.; Wang, H.; Deng, Y.-H.; Chen, M.-C.; Peng, L.-C.; Luo, Y.-H.; Qin, J.; Wu, D.; Ding, X.; Hu, Y.; Hu, P.; Yang, X.-Y.; Zhang, W.-J.; Li, H.; Li, Y.; Jiang, X.; Gan, L.; Yang, G.; You, L.; Wang, Z.; Li, L.; Liu, N.-L.; Lu, C.-Y.; Pan, J.-W. Quantum computational advantage using photons. *Science* **2020**, *370* (6523), 1460−1463.
(6) Blais, A.; Huang, R. S.; Wallraff, A.; Girvin, S. M.; Schoelkopf, R. J. Cavity quantum electrodynamics for superconducting electrical circuits: An architecture for quantum computation. *Phys. Rev. A* **2004**, *69* (6), No. 062320.
(7) Gaita-Arino, A.; Luis, F.; Hill, S.; Coronado, E. Molecular spins for quantum computation. *Nat. Chem.* **2019**, *11* (4), 301−309.
(8) Moreno-Da Silva, S.; Martinez, J. I.; Develioglu, A.; Nieto-Ortega, B.; de Juan-Fernandez, L.; Ruiz-Gonzalez, L.; Picon, A.; Oberli, S.; Alonso, P. J.; Moonshiram, D.; Perez, E. M.; Burzuri, E. Magnetic, Mechanically Interlocked Porphyrin-Carbon Nanotubes for Quantum Computation and Spintronics. *J. Am. Chem. Soc.* **2021**, *143* (50), 21286−21293.
(9) Kim, Y.; Eddins, A.; Anand, S.; Wei, K. X.; Van Den Berg, E.; Rosenblatt, S.; Nayfeh, H.; Wu, Y.; Zaletel, M.; Temme, K.; et al. Evidence for the utility of quantum computing before fault tolerance. *Nature* **2023**, *618* (7965), 500−505.
(10) Troiani, F.; Affronte, M. Molecular spins for quantum information technologies. *Chem. Soc. Rev.* **2011**, *40* (6), 3119−3129.
(11) Northup, T. E.; Blatt, R. Quantum information transfer using photons. *Nat. Photonics* **2014**, *8* (5), 356−363.
(12) Wasielewski, M. R.; Forbes, M. D. E.; Frank, N. L.; Kowalski, K.; Scholes, G. D.; Yuen-Zhou, J.; Baldo, M. A.; Freedman, D. E.; Goldsmith, R. H.; Goodson, T.; Kirk, M. L.; McCusker, J. K.; Ogilvie, J. P.; Shultz, D. A.; Stoll, S.; Whaley, K. B. Exploiting chemistry and molecular systems for quantum information science. *Nat. Rev. Chem.* **2020**, *4* (9), 490−504.
(13) Bayliss, S. L.; Laorenza, D. W.; Mintun, P. J.; Kovos, B. D.; Freedman, D. E.; Awschalom, D. D. Optically addressable molecular spins for quantum information processing. *Science* **2020**, *370* (6522), 1309−1312.
(14) Kimble, H. J. The quantum internet. *Nature* **2008**, *453* (7198), 1023−1030.
(15) Degen, C. L.; Reinhard, F.; Cappellaro, P. Quantum sensing. *Rev. Mod. Phys.* **2017**, *89* (3), No. 035002.
(16) Yu, C. J.; von Kugelgen, S.; Laorenza, D. W.; Freedman, D. E. A Molecular Approach to Quantum Sensing. *ACS Cent. Sci.* **2021**, *7* (5), 712−723.
(17) Pirandola, S.; Bardhan, B. R.; Gehring, T.; Weedbrook, C.; Lloyd, S. Advances in photonic quantum sensing. *Nat. Photonics* **2018**, *12*, 724−733.
(18) Kielpinski, D.; Monroe, C.; Wineland, D. J. Architecture for a large-scale ion-trap quantum computer. *Nature* **2002**, *417* (6890), 709−711.
(19) Monroe, C. R.; Wineland, D. J. Quantum computing with ions. *Sci. Am.* **2008**, *299* (2), 64−71.
(20) March, R. E. Quadrupole ion traps. *Mass Spectrom. Rev.* **2009**, *28* (6), 961−89.
(21) Nolting, D.; Malek, R.; Makarov, A. Ion traps in modern mass spectrometry. *Mass Spectrom. Rev.* **2019**, *38* (2), 150−168.
(22) Ebadi, S.; Wang, T. T.; Levine, H.; Keesling, A.; Semeghini, G.; Omran, A.; Bluvstein, D.; Samajdar, R.; Pichler, H.; Ho, W. W.; Choi, S.; Sachdev, S.; Greiner, M.; Vuletic, V.; Lukin, M. D. Quantum phases of matter on a 256-atom programmable quantum simulator. *Nature* **2021**, *595* (7866), 227−232.
(23) Graham, T. M.; Song, Y.; Scott, J.; Poole, C.; Phuttitarn, L.; Jooya, K.; Eichler, P.; Jiang, X.; Marra, A.; Grinkemeyer, B.; Kwon, M.; Ebert, M.; Cherek, J.; Lichtman, M. T.; Gillette, M.; Gilbert, J.; Bowman, D.; Ballance, T.; Campbell, C.; Dahl, E. D.; Crawford, O.; Blunt, N. S.; Rogers, B.; Noel, T.; Saffman, M. Multi-qubit entanglement and algorithms on a neutral-atom quantum computer. *Nature* **2022**, *604* (7906), 457−462.
(24) Nishida, S.; Morita, Y.; Fukui, K.; Sato, K.; Shiomi, D.; Takui, T.; Nakasuji, K. Spin transfer and solvato-/thermochromism induced by intramolecular electron transfer in a purely organic open-shell system. *Angew. Chem., Int. Ed.* **2005**, *44* (44), 7277−7280.
(25) Sato, K.; Nakazawa, S.; Rahimi, R.; Ise, T.; Nishida, S.; Yoshino, T.; Mori, N.; Toyota, K.; Shiomi, D.; Yakiyama, Y.; Morita, Y.; Kitagawa, M.; Nakasuji, K.; Nakahara, M.; Hara, H.; Carl, P.; Hofer, P.; Takui, T. Molecular electron-spin quantum computers and quantum information processing: pulse-based electron magnetic resonance spin technology applied to matter spin-qubits. *J. Mater. Chem.* **2009**, *19* (22), 3739−3754.
(26) Vincent, R.; Klyatskaya, S.; Ruben, M.; Wernsdorfer, W.; Balestro, F. Electronic read-out of a single nuclear spin using a molecular spin transistor. *Nature* **2012**, *488* (7411), 357−360.
(27) Narita, A.; Wang, X. Y.; Feng, X. L.; Mullen, K. New advances in nanographene chemistry. *Chem. Soc. Rev.* **2015**, *44* (18), 6616−6643.
(28) Yamamoto, S.; Nakazawa, S.; Sugisaki, K.; Sato, K.; Toyota, K.; Shiomi, D.; Takui, T. Adiabatic quantum computing with spin qubits

https://doi.org/10.1021/acs.jpclett.4c00264
J. Phys. Chem. Lett. 2024, 15, 3294−3316

hosted by molecules. *Phys. Chem. Chem. Phys.* **2015**, *17* (4), 2742−2749.
(29) Zadrozny, J. M.; Niklas, J.; Poluektov, O. G.; Freedman, D. E. Millisecond Coherence Time in a Tunable Molecular Electronic Spin Qubit. *ACS Cent. Sci.* **2015**, *1* (9), 488−492.
(30) Gallagher, N. M.; Bauer, J. J.; Pink, M.; Rajca, S.; Rajca, A. High-Spin Organic Diradical with Robust Stability. *J. Am. Chem. Soc.* **2016**, *138* (30), 9377−9380.
(31) Koehl, W. F.; Diler, B.; Whiteley, S. J.; Bourassa, A.; Son, N. T.; Janzen, E.; Awschalom, D. D. Resonant optical spectroscopy and coherent control of Cr4+ spin ensembles in SiC and GaN. *Phys. Rev. B* **2017**, *95* (3), No. 035207.
(32) Sproules, S. Molecules as electron spin qubits. *Electron Paramag. Reson.* **2016**, *25*, 61−97.
(33) Yamabayashi, T.; Atzori, M.; Tesi, L.; Cosquer, G.; Santanni, F.; Boulon, M. E.; Morra, E.; Benci, S.; Torre, R.; Chiesa, M.; Sorace, L.; Sessoli, R.; Yamashita, M. Scaling Up Electronic Spin Qubits into a Three-Dimensional Metal Organic Framework. *J. Am. Chem. Soc.* **2018**, *140* (38), 12090−12101.
(34) Poryvaev, A. S.; Gjuzi, E.; Polyukhov, D. M.; Hoffmann, F.; Froba, M.; Fedin, M. V. Blatter-Radical-Grafted Mesoporous Silica as Prospective Nanoplatform for Spin Manipulation at Ambient Conditions. *Angew. Chem., Int. Ed.* **2021**, *60* (16), 8683−8688.
(35) Hou, L.; Xu, H.; Zhang, X.; Chen, R.; Zhang, Z.; Wang, M.; et al. Impact of Polymer Rigidity on Thermoresponsive Luminescence and Electron Spin Resonance of Polyester-Tethered Single Radicals. *Macromolecules* **2022**, *55* (19), 8619−8628.
(36) Ayabe, K.; Sato, K.; Nishida, S.; Ise, T.; Nakazawa, S.; Sugisaki, K.; Morita, Y.; Toyota, K.; Shiomi, D.; Kitagawa, M.; Takui, T. Pulsed electron spin nutation spectroscopy of weakly exchange-coupled biradicals: a general theoretical approach and determination of the spin dipolar interaction. *Phys. Chem. Chem. Phys.* **2012**, *14* (25), 9137−9148.
(37) Li, J. C.; Merino-Diez, N.; Carbonell-Sanroma, E.; Vilas-Varela, M.; de Oteyza, D. G.; Pena, D.; Corso, M.; Pascual, J. I. Survival of spin state in magnetic porphyrins contacted by graphene nanoribbons. *Sci. Adv.* **2018**, *4* (2), No. eaaq0582.
(38) Y. Gopalakrishna, T.; Zeng, W.; Lu, X.; Wu, J. From open-shell singlet diradicaloids to polyradicaloids. *Chem. Commun.* **2018**, *54* (18), 2186−2199.
(39) Urtizberea, A.; Natividad, E.; Alonso, P. J.; Andres, M. A.; Gascon, I.; Goldmann, M.; Roubeau, O. A Porphyrin Spin Qubit and Its 2D Framework Nanosheets. *Adv. Funct. Mater.* **2018**, *28* (31), No. 1801695.
(40) Wang, D. Q.; Kelkar, H.; Martin-Cano, D.; Rattenbacher, D.; Shkarin, A.; Utikal, T.; Gotzinger, S.; Sandoghdar, V. Turning a molecule into a coherent two-level quantum system. *Nat. Phys.* **2019**, *15* (5), 483−489.
(41) Yu, C. J.; Krzyaniak, M. D.; Fataftah, M. S.; Wasielewski, M. R.; Freedman, D. E. A concentrated array of copper porphyrin candidate qubits. *Chem. Sci.* **2019**, *10* (6), 1702−1708.
(42) Bartos, P.; Anand, B.; Pietrzak, A.; Kaszynski, P. Functional Planar Blatter Radical through Pschorr-Type Cyclization. *Org. Lett.* **2020**, *22* (1), 180−184.
(43) Yu, C. J.; von Kugelgen, S.; Krzyaniak, M. D.; Ji, W.; Dichtel, W. R.; Wasielewski, M. R.; Freedman, D. E. Spin and Phonon Design in Modular Arrays of Molecular Qubits. *Chem. Mater.* **2020**, *32* (23), 10200−10206.
(44) Zhao, S.; Lavie, J.; Rondin, L.; Orcin-Chaix, L.; Diederichs, C.; Roussignol, P.; Chassagneux, Y.; Voisin, C.; Mullen, K.; Narita, A.; Campidelli, S.; Lauret, J. S. Single photon emission from graphene quantum dots at room temperature. *Nat. Commun.* **2018**, *9* (1), 3470.
(45) Alivisatos, A. P. Semiconductor clusters, nanocrystals, and quantum dots. *Science* **1996**, *271* (5251), 933−937.
(46) Lovric, J.; Bazzi, H. S.; Cuie, Y.; Fortin, G. R. A.; Winnik, F. M.; Maysinger, D. Differences in subcellular distribution and toxicity of green and red emitting CdTe quantum dots. *J. Mol. Med.* **2005**, *83* (5), 377−385.
(47) Lim, S. Y.; Shen, W.; Gao, Z. Carbon quantum dots and their applications. *Chem. Soc. Rev.* **2015**, *44* (1), 362−381.
(48) Das, R.; Bandyopadhyay, R.; Pramanik, P. Carbon quantum dots from natural resource: A review. *Mater. Today Chem.* **2018**, *8*, 96−109.
(49) Marquardt, F.; Bruder, C. Superposition of two mesoscopically distinct quantum states: Coupling a Cooper-pair box to a large superconducting island. *Phys. Rev. B* **2001**, *63*, No. 054516.
(50) Yang, C.; Chu, S.; Han, S. Possible realization of entanglement, logical gates, and quantum-information transfer with superconducting-quantum-interference-device qubits in cavity QED. *Phys. Rev. A* **2003**, *67*, No. 042311.
(51) Mariantoni, M.; Wang, H.; Yamamoto, T.; Neeley, M.; Bialczak, R. C.; Chen, Y.; Lenander, M.; Lucero, E.; O'Connell, A. D.; Sank, D.; Weides, M.; Wenner, J.; Yin, Y.; Zhao, J.; Korotkov, A. N.; Cleland, A. N.; Martinis, J. M. Implementing the quantum von Neumann architecture with superconducting circuits. *Science* **2011**, *334* (6052), 61−65.
(52) Mehra, J.; Rechenberg, H. *The Historical Development of Quantum Theory*; Springer: New York, 1982; Vol. *1*.
(53) Nolde, F.; Pisula, W.; Muller, S.; Kohl, C.; Mullen, K. Synthesis and self-organization of core-extended perylene tetracarboxdiimides with branched alkyl substituents. *Chem. Mater.* **2006**, *18* (16), 3715−3725.
(54) Bendikov, M.; Wudl, F.; Perepichka, D. F. Tetrathiafulvalenes, oligoacenenes, and their buckminsterfullerene derivatives: The brick and mortar of organic electronics. *Chem. Rev.* **2004**, *104* (11), 4891−4945.
(55) Anthony, J. E. The larger acenes: Versatile organic semiconductors. *Angew. Chem., Int. Ed.* **2008**, *47* (3), 452−483.
(56) Weller, H. Colloidal semiconductor q-particles: chemistry in the transition region between solid state and molecules. *Angew. Chem., Int. Ed.* **1993**, *32* (1), 41−53.
(57) Murray, C. B.; Kagan, C. R.; Bawendi, M. G. Synthesis and characterization of monodisperse nanocrystals and close-packed nanocrystal assemblies. *Annu. Rev. Mater. Sci.* **2000**, *30* (1), 545−610.
(58) Scholes, G. D.; Rumbles, G. Excitons in nanoscale systems. *Nat. Mater.* **2006**, *5* (9), 683−696.
(59) Empedocles, S. A.; Bawendi, M. G. Quantum-confined stark effect in single CdSe nanocrystallite quantum dots. *Science* **1997**, *278* (5346), 2114−7.
(60) Bawendi, M. G.; Steigerwald, M. L.; Brus, L. E. The quantum mechanics of larger semiconductor clusters (" quantum dots"). *Annu. Rev. Phys. Chem.* **1990**, *41* (1), 477−496.
(61) Ekimov, A. I.; Hache, F.; Schanne-Klein, M.; Ricard, D.; Flytzanis, C.; Kudryavtsev, I.; Yazeva, T.; Rodina, A.; Efros, A. L. Absorption and intensity-dependent photoluminescence measurements on CdSe quantum dots: assignment of the first electronic transitions. *JOSA B* **1993**, *10* (1), 100−107.
(62) Gaponik, N.; Talapin, D. V.; Rogach, A. L.; Hoppe, K.; Shevchenko, E. V.; Kornowski, A.; Eychmuller, A.; Weller, H. Thiol-capping of CdTe nanocrystals: An alternative to organometallic synthetic routes. *J. Phys. Chem. B* **2002**, *106* (29), 7177−7185.
(63) Rogach, A. L.; Franzl, T.; Klar, T. A.; Feldmann, J.; Gaponik, N.; Lesnyak, V.; Shavel, A.; Eychmuller, A.; Rakovich, Y. P.; Donegan, J. F. Aqueous synthesis of thiol-capped CdTe nanocrystals: State-of-the-art. *J. Phys. Chem. C* **2007**, *111* (40), 14628−14637.
(64) Tsoi, K. M.; Dai, Q.; Alman, B. A.; Chan, W. C. Are quantum dots toxic? Exploring the discrepancy between cell culture and animal studies. *Acc. Chem. Res.* **2013**, *46* (3), 662−671.
(65) Gao, M. Y.; Lesser, C.; Kirstein, S.; Mohwald, H.; Rogach, A. L.; Weller, H. Electroluminescence of different colors from polycation/CdTe nanocrystal self-assembled films. *J. Appl. Phys.* **2000**, *87* (5), 2297−2302.
(66) Dai, X.; Zhang, Z.; Jin, Y.; Niu, Y.; Cao, H.; Liang, X.; Chen, L.; Wang, J.; Peng, X. Solution-processed, high-performance light-emitting diodes based on quantum dots. *Nature* **2014**, *515* (7525), 96−99.

https://doi.org/10.1021/acs.jpclett.4c00264
J. Phys. Chem. Lett. 2024, 15, 3294−3316

(67) Chen, X.; Lu, W.-g.; Tang, J.; Zhang, Y.; Wang, Y.; Scholes, G. D.; Zhong, H. Solution-processed inorganic perovskite crystals as achromatic quarter-wave plates. *Nat. Photonics* **2021**, *15* (11), 813−816.
(68) Lu, C.-Y.; Pan, J.-W. Quantum-dot single-photon sources for the quantum internet. *Nat. Nanotechnol.* **2021**, *16* (12), 1294−1296.
(69) Yang, J.; Chen, Y.; Rao, Z.; Zheng, Z.; Song, C.; Chen, Y.; Xiong, K.; Chen, P.; Zhang, C.; Wu, W.; et al. Tunable quantum dots in monolithic Fabry-Perot microcavities for high-performance single-photon sources. *Light Sci. Appl.* **2024**, *13* (1), 33.
(70) Hanson, R.; Kouwenhoven, L. P.; Petta, J. R.; Tarucha, S.; Vandersypen, L. M. Spins in few-electron quantum dots. *Rev. Mod. Phys.* **2007**, *79* (4), 1217.
(71) Mortemousque, P.-A.; Chanrion, E.; Jadot, B.; Flentje, H.; Ludwig, A.; Wieck, A. D.; Urdampilleta, M.; Bäuerle, C.; Meunier, T. Coherent control of individual electron spins in a two-dimensional quantum dot array. *Nat. Nanotechnol.* **2021**, *16* (3), 296−301.
(72) Uppu, R.; Midolo, L.; Zhou, X.; Carolan, J.; Lodahl, P. Quantum-dot-based deterministic photon−emitter interfaces for scalable photonic quantum technology. *Nat. Nanotechnol.* **2021**, *16* (12), 1308−1317.
(73) Borsoi, F.; Hendrickx, N. W.; John, V.; Meyer, M.; Motz, S.; Van Riggelen, F.; Sammak, A.; De Snoo, S. L.; Scappucci, G.; Veldhorst, M. Shared control of a 16 semiconductor quantum dot crossbar array. *Nat. Nanotechnol.* **2024**, *19* (1), 21−27.
(74) Mirkovic, T.; Ostroumov, E. E.; Anna, J. M.; van Grondelle, R.; Govindjee; Scholes, G. D. Light Absorption and Energy Transfer in the Antenna Complexes of Photosynthetic Organisms. *Chem. Rev.* **2017**, *117* (2), 249−293.
(75) Fleming, G. R.; Scholes, G. D. Quantum biology: introduction. In *Quantum Effects in Biology*; Cambridge University Press: Cambridge, 2014.
(76) Scholes, G. D. Quantum-Coherent Electronic Energy Transfer: Did Nature Think of It First? *J. Phys. Chem. Lett.* **2010**, *1* (1), 2−8.
(77) Ma, S. Q.; Du, S. J.; Pan, G. C.; Dai, S. T.; Xu, B.; Tian, W. J. Organic molecular aggregates: From aggregation structure to emission property. *Aggregate* **2021**, *2* (4), No. e96.
(78) Wurthner, F.; Kaiser, T. E.; Saha-Möller, C. R. J-aggregates: from serendipitous discovery to supramolecular engineering of functional dye materials. *Angew. Chem., Int. Ed.* **2011**, *50* (15), 3376−3410.
(79) Mei, J.; Leung, N. L. C.; Kwok, R. T. K.; Lam, J. W. Y.; Tang, B. Z. Aggregation-Induced Emission: Together We Shine, United We Soar. *Chem. Rev.* **2015**, *115* (21), 11718−11940.
(80) Knapp, E. W. Lineshapes of Molecular Aggregates - Exchange Narrowing and Intersite Correlation. *Chem. Phys.* **1984**, *85* (1), 73−82.
(81) Hestand, N. J.; Spano, F. C. Expanded Theory of H- and J-Molecular Aggregates: The Effects of Vibronic Coupling and Intermolecular Charge Transfer. *Chem. Rev.* **2018**, *118* (15), 7069−7163.
(82) Humeniuk, A.; Mitric, R.; Bonacic-Koutecky, V. Size Dependence of Non-Radiative Decay Rates in J-Aggregates. *J. Phys. Chem. A* **2020**, *124* (49), 10143−10151.
(83) Zhang, Y.; Lou, H.; Wang, M. Kinetic and Thermodynamic Control of Supramolecular Aggregation of Near Infrared Pyrrolopyrrole Cyanine Fluorophores Confined in Colloidal Nanoparticles. *Chem. Eur. J.* **2024**, *30*, No. e202303204.
(84) Kim, J. H.; Schembri, T.; Bialas, D.; Stolte, M.; Würthner, F. Slip-Stacked J-Aggregate Materials for Organic Solar Cells and Photodetectors. *Adv. Mater.* **2022**, *34* (22), No. e2104678.
(85) Kasha, M.; Rawls, H. R.; Ashraf El-Bayoumi, M. The exciton model in molecular spectroscopy. *Pure Appl. Chem.* **1965**, *11* (3−4), 371−392.
(86) Huber, V.; Sengupta, S.; Wurthner, F. Structure-property relationships for self-assembled zinc chlorin light-harvesting dye aggregates. *Chem.—Eur. J.* **2008**, *14* (26), 7791−7807.
(87) Holzwarth, A. R.; Schaffner, K. On the Structure of Bacteriochlorophyll Molecular Aggregates in the Chlorosomes of Green Bacteria - a Molecular Modeling Study. *Photosyn. Res.* **1994**, *41* (1), 225−233.
(88) Kemnitz, K.; Yoshihara, K.; Tani, T. Short and Excitation-Independent Fluorescence Lifetimes of J-Aggregates Adsorbed on Agbr and Sio2. *J. Phys. Chem.* **1990**, *94* (7), 3099−3104.
(89) Psencik, J.; Polivka, T.; Nemec, P.; Dian, J.; Kudrna, J.; Maly, P.; Hala, J. Fast energy transfer and exciton dynamics in chlorosomes of the green sulfur bacterium Chlorobium tepidum. *J. Phys. Chem. A* **1998**, *102* (23), 4392−4398.
(90) Schoelkopf, R. J.; Girvin, S. M. Wiring up quantum systems. *Nature* **2008**, *451* (7179), 664−669.
(91) de Leon, N. P.; Itoh, K. M.; Kim, D.; Mehta, K. K.; Northup, T. E.; Paik, H.; Palmer, B. S.; Samarth, N.; Sangtawesin, S.; Steuerman, D. W. Materials challenges and opportunities for quantum computing hardware. *Science* **2021**, *372* (6539), No. eabb2823.
(92) Monroe, C.; Kim, J. Scaling the Ion Trap Quantum Processor. *Science* **2013**, *339* (6124), 1164−1169.
(93) Brownnutt, M.; Kumph, M.; Rabl, P.; Blatt, R. Ion-trap measurements of electric-field noise near surfaces. *Rev. Mod. Phys.* **2015**, *87* (4), 1419−1482.
(94) Romaszko, Z. D.; Hong, S.; Siegele, M.; Puddy, R. K.; Lebrun-Gallagher, F. R.; Weidt, S.; Hensinger, W. K. Engineering of microfabricated ion traps and integration of advanced on-chip features. *Nat. Rev. Phys.* **2020**, *2* (6), 285−299.
(95) Atzori, M.; Sessoli, R. The Second Quantum Revolution: Role and Challenges of Molecular Chemistry. *J. Am. Chem. Soc.* **2019**, *141* (29), 11339−11352.
(96) Atature, M.; Englund, D.; Vamivakas, N.; Lee, S. Y.; Wrachtrup, J. Material platforms for spin-based photonic quantum technologies. *Nat. Rev. Mater.* **2018**, *3* (5), 38−51.
(97) Lambert, N.; Chen, Y. N.; Cheng, Y. C.; Li, C. M.; Chen, G. Y.; Nori, F. Quantum biology. *Nat. Phys.* **2013**, *9* (1), 10−18.
(98) Proppe, A. H.; Li, Y. G. C.; Aspuru-Guzik, A.; Berlinguette, C. P.; Chang, C. J.; Cogdell, R.; Doyle, A. G.; Flick, J.; Gabor, N. M.; van Grondelle, R.; Hammes-Schiffer, S.; Jaffer, S. A.; Kelley, S. O.; Leclerc, M.; Leo, K.; Mallouk, T. E.; Narang, P.; Schlau-Cohen, G. S.; Scholes, G. D.; Vojvodic, A.; Yam, V. W. W.; Yang, J. Y.; Sargent, E. H. Bioinspiration in light harvesting and catalysis. *Nat. Rev. Mater.* **2020**, *5* (11), 828−846.
(99) Bennett, C. H.; DiVincenzo, D. P. Quantum information and computation. *Nature* **2000**, *404* (6775), 247−255.
(100) Acin, A.; Bloch, I.; Buhrman, H.; Calarco, T.; Eichler, C.; Eisert, J.; Esteve, D.; Gisin, N.; Glaser, S. J.; Jelezko, F.; Kuhr, S.; Lewenstein, M.; Riedel, M. F.; Schmidt, P. O.; Thew, R.; Wallraff, A.; Walmsley, I.; Wilhelm, F. K. The quantum technologies roadmap: a European community view. *New J. Phys.* **2018**, *20* (8), No. 080201.
(101) Mohseni, M.; Read, P.; Neven, H.; Boixo, S.; Denchev, V.; Babbush, R.; Fowler, A.; Smelyanskiy, V.; Martinis, J. Commercialize early quantum technologies. *Nature* **2017**, *543* (7644), 171−174.
(102) Ladd, T. D.; Jelezko, F.; Laflamme, R.; Nakamura, Y.; Monroe, C.; O'Brien, J. L. Quantum computers. *Nature* **2010**, *464* (7285), 45−53.
(103) Tokura, Y.; Kawasaki, M.; Nagaosa, N. Emergent functions of quantum materials. *Nat. Phys.* **2017**, *13* (11), 1056−1068.
(104) Wolf, S. A.; Awschalom, D. D.; Buhrman, R. A.; Daughton, J. M.; von Molnar, S.; Roukes, M. L.; Chtchelkanova, A. Y.; Treger, D. M. Spintronics: A spin-based electronics vision for the future. *Science* **2001**, *294* (5546), 1488−1495.
(105) O'Brien, J. L. Optical quantum computing. *Science* **2007**, *318* (5856), 1567−1570.
(106) Scholes, G. D. A Molecular Perspective on Quantum Information. *Proc. R. Soc. A* **2023**, *479*, No. 20230599.
(107) Glauber, R. J. Photon correlations. *Phys. Rev. Lett.* **1963**, *10* (3), 84.
(108) Barnett, S. *Quantum information*; Oxford University Press: Oxford, 2009; Vol. *16*.
(109) Pezzagna, S.; Meijer, J. Quantum computer based on color centers in diamond. *Appl. Phys. Rev.* **2021**, *8* (1), No. 011308.

https://doi.org/10.1021/acs.jpclett.4c00264
J. Phys. Chem. Lett. 2024, 15, 3294−3316

(110) Bluvstein, D.; Omran, A.; Levine, H.; Keesling, A.; Semeghini, G.; Ebadi, S.; Wang, T. T.; Michailidis, A. A.; Maskara, N.; Ho, W. W.; Choi, S.; Serbyn, M.; Greiner, M.; Vuletic, V.; Lukin, M. D. Controlling quantum many-body dynamics in driven Rydberg atom arrays. *Science* **2021**, *371* (6536), 1355−1359.
(111) Castelletto, S.; Boretti, A. Silicon carbide color centers for quantum applications. *J. Phys. Photonics* **2020**, *2* (2), No. 022001.
(112) Wrachtrup, J.; Vonborczyskowski, C.; Bernard, J.; Orrit, M.; Brown, R. Optical-Detection of Magnetic-Resonance in a Single Molecule. *Nature* **1993**, *363* (6426), 244−245.
(113) Berliner, L. J. *In vivo EPR (ESR): theory and application*; Kluwer Academic/Plenum Publishers: New York, 2003.
(114) Jackson, C. E.; Lin, C. Y.; Johnson, S. H.; van Tol, J.; Zadrozny, J. M. Nuclear-spin-pattern control of electron-spin dynamics in a series of V(iv) complexes. *Chem. Sci.* **2019**, *10* (36), 8447−8454.
(115) Oxborrow, M.; Breeze, J. D.; Alford, N. M. Room-temperature solid-state maser. *Nature* **2012**, *488* (7411), 353−356.
(116) Nakazawa, S.; Nishida, S.; Ise, T.; Yoshino, T.; Mori, N.; Rahimi, R. D.; Sato, K.; Morita, Y.; Toyota, K.; Shiomi, D.; Kitagawa, M.; Hara, H.; Carl, P.; Hofer, P.; Takui, T. A Synthetic Two-Spin Quantum Bit: g-Engineered Exchange-Coupled Biradical Designed for Controlled-NOT Gate Operations. *Angew. Chem., Int. Ed.* **2012**, *51* (39), 9860−9864.
(117) Karoui, H.; Moigne, F. L.; Ouari, O.; Tordo, P. *Stable radicals: Fundamentals and Applied Aspects of Odd-Electron Compounds*; Wiley: Chichester, UK, 2010.
(118) Suzuki, S.; Nagata, A.; Kuratsu, M.; Kozaki, M.; Tanaka, R.; Shiomi, D.; Sugisaki, K.; Toyota, K.; Sato, K.; Takui, T.; Okada, K. Trinitroxide-Trioxytriphenylamine: Spin-State Conversion from Triradical Doublet to Diradical Cation Triplet by Oxidative Modulation of a p-Conjugated System. *Angew. Chem., Int. Ed.* **2012**, *51* (13), 3193−3197.
(119) Yoshino, T.; Nishida, S.; Sato, K.; Nakazawa, S.; Rahimi, R. D.; Toyota, K.; Shiomi, D.; Morita, Y.; Kitagawa, M.; Takui, T. ESR and H-1-, F-19-ENDOR/TRIPLE Study of Fluorinated Diphenylnitroxides as Synthetic Bus Spin-Qubit Radicals with Client Qubits in Solution. *J. Phys. Chem. Lett.* **2011**, *2* (5), 449−453.
(120) Morita, Y.; Suzuki, S.; Sato, K.; Takui, T. Synthetic organic spin chemistry for structurally well-defined open-shell graphene fragments. *Nat. Chem.* **2011**, *3* (3), 197−204.
(121) Ueda, A.; Suzuki, S.; Yoshida, K.; Fukui, K.; Sato, K.; Takui, T.; Nakasuji, K.; Morita, Y. Hexamethoxyphenalenyl as a Possible Quantum Spin Simulator: An Electronically Stabilized Neutral pi Radical with Novel Quantum Coherence Owing to Extremely High Nuclear Spin Degeneracy. *Angew. Chem., Int. Ed.* **2013**, *52* (18), 4795−4799.
(122) Ueda, A.; Wasa, H.; Suzuki, S.; Okada, K.; Sato, K.; Takui, T.; Morita, Y. Chiral Stable Phenalenyl Radical: Synthesis, Electronic-Spin Structure, and Optical Properties of [4]Helicene-Structured Diazaphenalenyl. *Angew. Chem., Int. Ed.* **2012**, *51* (27), 6691−6695.
(123) Lombardi, F.; Lodi, A.; Ma, J.; Liu, J. Z.; Slota, M.; Narita, A.; Myers, W. K.; Mullen, K.; Feng, X. L.; Bogani, L. Quantum units from the topological engineering of molecular graphenoids. *Science* **2019**, *366* (6469), 1107−1110.
(124) Constantinides, C. P.; Koutentis, P. A.; Krassos, H.; Rawson, J. M.; Tasiopoulos, A. J. Characterization and Magnetic Properties of a "Super Stable" Radical 1,3-Diphenyl-7-trifluoromethyl-1,4-dihydro-1,2,4-benzotriazin-4-yl. *J. Org. Chem.* **2011**, *76* (8), 2798−2806.
(125) Ji, Y.; Long, L. X.; Zheng, Y. H. Recent advances of stable Blatter radicals: synthesis, properties and applications. *Mater. Chem. Front.* **2020**, *4* (12), 3433−3443.
(126) Affronte, M.; Casson, I.; Evangelisti, M.; Candini, A.; Carretta, S.; Muryn, C.; Teat, S. J.; Timco, G. A.; Wernsdorfer, W.; Winpenny, R. E. P. Linking rings through diamines and clusters: Exploring synthetic methods for making magnetic quantum gates. *Angew. Chem., Int. Ed.* **2005**, *44* (40), 6496−6500.
(127) Zhou, S.; Yuan, J.; Wang, Z. Y.; Ling, K.; Fu, P. X.; Fang, Y. H.; Wang, Y. X.; Liu, Z.; Porfyrakis, K.; Briggs, G. A. D.; et al. Implementation of quantum level addressability and geometric phase manipulation in aligned endohedral fullerene qudits. *Angew. Chem., Int. Ed.* **2022**, *61* (8), No. e202115263.
(128) Fu, P. X.; Zhou, S.; Liu, Z.; Wu, C. H.; Fang, Y. H.; Wu, Z. R.; Tao, X. Q.; Yuan, J. Y.; Wang, Y. X.; Gao, S. Multiprocessing Quantum Computing through Hyperfine Couplings in Endohedral Fullerene Derivatives. *Angew. Chem., Int. Ed.* **2022**, *61* (52), No. e202212939.
(129) Morton, J. J. L.; Tyryshkin, A. M.; Ardavan, A.; Porfyrakis, K.; Lyon, S. A.; Briggs, G. A. D. Electron spin relaxation of N@C-60 in CS2. *J. Chem. Phys.* **2006**, *124* (1), No. 014508.
(130) Hu, Z. Q.; Dong, B. W.; Liu, Z.; Liu, J. J.; Yu, C. C.; Xiong, J.; Shi, D. E.; Wang, Y. Y.; Wang, B. W.; Ardavan, A.; Shi, Z. J.; Jiang, S. D.; Gao, S. Endohedral Metallofullerene as Molecular High Spin Qubit: Diverse Rabi Cycles in Gd-2@C79N. *J. Am. Chem. Soc.* **2018**, *140* (3), 1123−1130.
(131) Dai, Y. Z.; Dong, B. W.; Kao, Y.; Wang, Z. Y.; Un, H. I.; Liu, Z.; Lin, Z. J.; Li, L.; Xie, F. B.; Lu, Y.; Xu, M. X.; Lei, T.; Sun, Y. J.; Wang, J. Y.; Gao, S.; Jiang, S. D.; Pei, J. Chemical Modification toward Long Spin Lifetimes in Organic Conjugated Radicals. *ChemPhysChem* **2018**, *19* (22), 2972−2977.
(132) Kato, K.; Kimura, S.; Kusamoto, T.; Nishihara, H.; Teki, Y. Luminescent Radical-Excimer: Excited-State Dynamics of Luminescent Radicals in Doped Host Crystals. *Angew. Chem., Int. Ed.* **2019**, *58* (9), 2606−2611.
(133) Gorgon, S.; Lv, K.; Grune, J.; Drummond, B. H.; Myers, W. K.; Londi, G.; Ricci, G.; Valverde, D.; Tonnele, C.; Murto, P.; Romanov, A. S.; Casanova, D.; Dyakonov, V.; Sperlich, A.; Beljonne, D.; Olivier, Y.; Li, F.; Friend, R. H.; Evans, E. W. Reversible spin-optical interface in luminescent organic radicals. *Nature* **2023**, *620* (7974), 538−544.
(134) Hou, L.; Zhang, Y.; Zhang, Y.; Jiang, S.-D.; Wang, M. Tunable quantum coherence of organic luminescent radical qubits centered in star-like block copolymers and self-assembling nanostructures. *ChemRxiv* **2023**, DOI: 10.26434/chemrxiv-2023-9z1jc.
(135) von Kugelgen, S.; Krzyaniak, M. D.; Gu, M.; Puggioni, D.; Rondinelli, J. M.; Wasielewski, M. R.; Freedman, D. E. Spectral Addressability in a Modular Two Qubit System. *J. Am. Chem. Soc.* **2021**, *143* (21), 8069−8077.
(136) Warner, M.; Din, S.; Tupitsyn, I. S.; Morley, G. W.; Stoneham, A. M.; Gardener, J. A.; Wu, Z. L.; Fisher, A. J.; Heutz, S.; Kay, C. W. M.; Aeppli, G. Potential for spin-based information processing in a thin-film molecular semiconductor. *Nature* **2013**, *503* (7477), 504−508.
(137) Graham, M. J.; Zadrozny, J. M.; Fataftah, M. S.; Freedman, D. E. Forging Solid-State Qubit Design Principles in a Molecular Furnace. *Chem. Mater.* **2017**, *29*, 1885−1897.
(138) Hua, C.; Baldansuren, A.; Tuna, F.; Collison, D.; D'Alessandro, D. M. In Situ Spectroelectrochemical Investigations of the Redox-Active Tris[4-(pyridin-4-yl)phenyl]amine Ligand and a Zn(2+) Coordination Framework. *Inorg. Chem.* **2016**, *55* (15), 7270−80.
(139) Kim, Y.; Koo, J.; Hwang, I. C.; Mukhopadhyay, R. D.; Hong, S.; Yoo, J.; Dar, A. A.; Kim, I.; Moon, D.; Shin, T. J.; Ko, Y. H.; Kim, K. Rational Design and Construction of Hierarchical Superstructures Using Shape-Persistent Organic Cages: Porphyrin Box-Based Metallosupramolecular Assemblies. *J. Am. Chem. Soc.* **2018**, *140* (44), 14547−14551.
(140) Fleming, G. R.; Scholes, G. D.; Cheng, Y.-C. Quantum effects in biology. *Procedia Chem.* **2011**, *3* (1), 38−57.
(141) Wiltschko, W.; Wiltschko, R. Magnetic compass of European robins. *Science* **1972**, *176* (4030), 62−64.
(142) Wiltschko, R.; Stapput, K.; Thalau, P.; Wiltschko, W. Directional orientation of birds by the magnetic field under different light conditions. *J. R. Soc. Interface* **2010**, *7*, S163−S177.
(143) Johnsen, S.; Lohmann, K. J. Magnetoreception in animals feature article. *Phys. Today* **2008**, *61* (3), 29−35.
(144) Ritz, T.; Adem, S.; Schulten, K. A model for photoreceptor-based magnetoreception in birds. *Biophys. J.* **2000**, *78* (2), 707−718.

https://doi.org/10.1021/acs.jpclett.4c00264
J. Phys. Chem. Lett. 2024, 15, 3294−3316

(145) Keary, N.; Ruploh, T.; Voss, J.; Thalau, P.; Wiltschko, R.; Wiltschko, W.; Bischof, H. J. Oscillating magnetic field disrupts magnetic orientation in Zebra finches, Taeniopygia guttata. *Front. Zool.* **2009**, *6*, 25.
(146) Ritz, T.; Wiltschko, R.; Hore, P. J.; Rodgers, C. T.; Stapput, K.; Thalau, P.; Timmel, C. R.; Wiltschko, W. Magnetic Compass of Birds Is Based on a Molecule with Optimal Directional Sensitivity. *Biophys. J.* **2009**, *96* (8), 3451−3457.
(147) Wiltschko, W.; Wiltschko, R. Magnetic compass orientation in birds and its physiological basis. *Sci. Nat.* **2002**, *89* (10), 445−452.
(148) Zapka, M.; Heyers, D.; Hein, C. M.; Engels, S.; Schneider, N.-L.; Hans, J.; Weiler, S.; Dreyer, D.; Kishkinev, D.; Wild, J. M.; Mouritsen, H. Visual but not trigeminal mediation of magnetic compass information in a migratory bird. *Nature* **2009**, *461* (7268), 1274−1277.
(149) Ritz, T.; Thalau, P.; Phillips, J. B.; Wiltschko, R.; Wiltschko, W. Resonance effects indicate a radical-pair mechanism for avian magnetic compass. *Nature* **2004**, *429* (6988), 177−180.
(150) Gauger, E. M.; Rieper, E.; Morton, J. J. L.; Benjamin, S. C.; Vedral, V. Sustained Quantum Coherence and Entanglement in the Avian Compass. *Phys. Rev. Lett.* **2011**, *106* (4), No. 040503.
(151) Rodgers, C. T.; Hore, P. J. Chemical magnetoreception in birds: The radical pair mechanism. *Proc. Natl. Acad. Sci. U.S.A.* **2009**, *106* (2), 353−360.
(152) Ghezzi, D.; Antognazza, M. R.; Maccarone, R.; Bellani, S.; Lanzarini, E.; Martino, N.; Mete, M.; Pertile, G.; Bisti, S.; Lanzani, G.; Benfenati, F. A polymer optoelectronic interface restores light sensitivity in blind rat retinas. *Nat. Photonics* **2013**, *7* (5), 400−406.
(153) Wu, Y.; Peng, Y.; Bohra, H.; Zou, J.; Ranjan, V. D.; Zhang, Y.; Zhang, Q.; Wang, M. Photoconductive Micro/Nanoscale Interfaces of a Semiconducting Polymer for Wireless Stimulation of Neuron-Like Cells. *ACS Appl. Mater. Interfaces* **2019**, *11* (5), 4833−4841.
(154) Huynh, M. H. V.; Meyer, T. J. Proton-coupled electron transfer. *Chem. Rev.* **2007**, *107* (11), 5004−5064.
(155) Nagel, Z. D.; Klinman, J. P. Tunneling and dynamics in enzymatic hydride transfer. *Chem. Rev.* **2006**, *106* (8), 3095−3118.
(156) Sen, A.; Kohen, A. Enzymatic tunneling and kinetic isotope effects: chemistry at the crossroads. *J. Phys. Chem. Lett.* **2010**, *23* (7), 613−619.
(157) Maeda, K.; Henbest, K. B.; Cintolesi, F.; Kuprov, I.; Rodgers, C. T.; Liddell, P. A.; Gust, D.; Timmel, C. R.; Hore, P. J. Chemical compass model of avian magnetoreception. *Nature* **2008**, *453* (7193), 387−390.
(158) Kuciauskas, D.; Liddell, P. A.; Moore, A. L.; Moore, T. A.; Gust, D. Magnetic switching of charge separation lifetimes in artificial photosynthetic reaction centers. *J. Am. Chem. Soc.* **1998**, *120* (42), 10880−10886.
(159) Liddell, P. A.; Kuciauskas, D.; Sumida, J. P.; Nash, B.; Nguyen, D.; Moore, A. L.; Moore, T. A.; Gust, D. Photoinduced charge separation and charge recombination to a triplet state in a carotene-porphyrin-fullerene triad. *J. Am. Chem. Soc.* **1997**, *119* (6), 1400−1405.
(160) Timmel, C. R.; Till, U.; Brocklehurst, B.; McLauchlan, K. A.; Hore, P. J. Effects of weak magnetic fields on free radical recombination reactions. *Mol. Phys.* **1998**, *95* (1), 71−89.
(161) Rodgers, C. T.; Norman, S. A.; Henbest, K. B.; Timmel, C. R.; Hore, P. J. Determination of radical re-encounter probability distributions from magnetic field effects on reaction yields. *J. Am. Chem. Soc.* **2007**, *129* (21), 6746−6755.
(162) Kerpal, C.; Richert, S.; Storey, J. G.; Pillai, S.; Liddell, P. A.; Gust, D.; Mackenzie, S. R.; Hore, P.; Timmel, C. R. Chemical compass behaviour at microtesla magnetic fields strengthens the radical pair hypothesis of avian magnetoreception. *Nat. Commun.* **2019**, *10* (1), 3707.
(163) Zhang, Y.; Hu, Z.; Wang, Y.; Kais, S. Quantum simulation of the radical pair dynamics of the avian compass. *J. Phys. Chem. Lett.* **2023**, *14* (3), 832−837.
(164) Babcock, N. S.; Kattnig, D. R. Radical scavenging could answer the challenge posed by electron−electron dipolar interactions in the cryptochrome compass model. *JACS Au* **2021**, *1* (11), 2033−2046.
(165) Solov'yov, I. A.; Chandler, D. E.; Schulten, K. Magnetic field effects in Arabidopsis thaliana cryptochrome-1. *Biophys. J.* **2007**, *92* (8), 2711−2726.
(166) Dodson, C. A.; Hore, P. J.; Wallace, M. I. A radical sense of direction: signalling and mechanism in cryptochrome magnetoreception. *Trends Biochem. Sci.* **2013**, *38* (9), 435−446.
(167) Maeda, K.; Robinson, A. J.; Henbest, K. B.; Hogben, H. J.; Biskup, T.; Ahmad, M.; Schleicher, E.; Weber, S.; Timmel, C. R.; Hore, P. J. Magnetically sensitive light-induced reactions in cryptochrome are consistent with its proposed role as a magnetoreceptor. *Proc. Natl. Acad. Sci. U.S.A.* **2012**, *109* (13), 4774−4779.
(168) Evans, E. W.; Kattnig, D. R.; Henbest, K. B.; Hore, P. J.; Mackenzie, S. R.; Timmel, C. R. Sub-millitesla magnetic field effects on the recombination reaction of flavin and ascorbic acid radicals. *J. Chem. Phys.* **2016**, *145* (8), No. 085101.
(169) Krzyaniak, M. D.; Kobr, L.; Rugg, B. K.; Phelan, B. T.; Margulies, E. A.; Nelson, J. N.; Young, R. M.; Wasielewski, M. R. Fast photo-driven electron spin coherence transfer: the effect of electron-nuclear hyperfine coupling on coherence dephasing. *J. Mater. Chem. C* **2015**, *3* (30), 7962−7967.
(170) Rugg, B. K.; Krzyaniak, M. D.; Phelan, B. T.; Ratner, M. A.; Young, R. M.; Wasielewski, M. R. Photodriven quantum teleportation of an electron spin state in a covalent donor−acceptor−radical system. *Nat. Chem.* **2019**, *11* (11), 981−986.
(171) Harvey, S. M.; Wasielewski, M. R. Photogenerated spin-correlated radical pairs: From photosynthetic energy transduction to quantum information science. *J. Am. Chem. Soc.* **2021**, *143* (38), 15508−15529.
(172) Pirandola, S.; Eisert, J.; Weedbrook, C.; Furusawa, A.; Braunstein, S. L. Advances in quantum teleportation. *Nat. Photonics* **2015**, *9* (10), 641−652.
(173) Rugg, B. K.; Krzyaniak, M. D.; Phelan, B. T.; Ratner, M. A.; Young, R. M.; Wasielewski, M. R. Photodriven quantum teleportation of an electron spin state in a covalent donor-acceptor-radical system. *Nat. Chem.* **2019**, *11* (11), 981−986.
(174) Stein, B. W.; Tichnell, C. R.; Chen, J.; Shultz, D. A.; Kirk, M. L. Excited state magnetic exchange interactions enable large spin polarization effects. *J. Am. Chem. Soc.* **2018**, *140* (6), 2221−2228.
(175) Hou, Y.; Kurganskii, I.; Elmali, A.; Zhang, H.; Gao, Y.; Lv, L.; Zhao, J.; Karatay, A.; Luo, L.; Fedin, M. Electronic coupling and spin−orbit charge transfer intersystem crossing (SOCT-ISC) in compact BDP−carbazole dyads with different mutual orientations of the electron donor and acceptor. *J. Chem. Phys.* **2020**, *152* (11), 114701.
(176) Ran, G.; Zeb, J.; Lu, H.; Liu, Y.; Zhang, A.; Wang, L.; Bo, Z.; Zhang, W. Ultrafast carrier dynamics of non-fullerene acceptors with different planarity: impact of steric hindrance. *J. Phys. Chem. Lett.* **2022**, *13* (25), 5860−5866.
(177) Caruso, F.; Atalla, V.; Ren, X.; Rubio, A.; Scheffler, M.; Rinke, P. First-principles description of charge transfer in donor-acceptor compounds from self-consistent many-body perturbation theory. *Phys. Rev. B* **2014**, *90* (8), No. 085141.
(178) Guzman, C. X.; Calderon, R. M. K.; Li, Z.; Yamazaki, S.; Peurifoy, S. R.; Guo, C.; Davidowski, S. K.; Mazza, M. M.; Han, X.; Holland, G.; et al. Extended charge carrier lifetimes in hierarchical donor−acceptor supramolecular polymer films. *J. Phys. Chem. C* **2015**, *119* (34), 19584−19589.
(179) Engel, G. S.; Calhoun, T. R.; Read, E. L.; Ahn, T. K.; Mancal, T.; Cheng, Y. C.; Blankenship, R. E.; Fleming, G. R. Evidence for wavelike energy transfer through quantum coherence in photosynthetic systems. *Nature* **2007**, *446* (7137), 782−786.
(180) Collini, E.; Wong, C. Y.; Wilk, K. E.; Curmi, P. M. G.; Brumer, P.; Scholes, G. D. Coherently wired light-harvesting in photosynthetic marine algae at ambient temperature. *Nature* **2010**, *463* (7281), 644−648.

https://doi.org/10.1021/acs.jpclett.4c00264
J. Phys. Chem. Lett. 2024, 15, 3294−3316

(181) Scholes, G. D.; Fleming, G. R.; Olaya-Castro, A.; van Grondelle, R. Lessons from nature about solar light harvesting. *Nat. Chem.* **2011**, *3* (10), 763−774.
(182) Jendrny, M.; Aartsma, T. J.; Kohler, J. Fluorescence Excitation Spectra from Individual Chlorosomes of the Green Sulfur Bacterium Chlorobaculum tepidum. *J. Phys. Chem. Lett.* **2012**, *3* (24), 3745−3750.
(183) Bohm, P. S.; Southall, J.; Cogdell, R. J.; Kohler, J. Single-Molecule Spectroscopy on RC-LH1 Complexes of Rhodopseudomonas acidophila Strain 10050. *J. Phys. Chem. B* **2013**, *117* (11), 3120−3126.
(184) Orf, G. S.; Blankenship, R. E. Chlorosome antenna complexes from green photosynthetic bacteria. *Photosyn. Res.* **2013**, *116* (2−3), 315−331.
(185) Shibata, Y.; Saga, Y.; Tamiaki, H.; Itoh, S. Anisotropic distribution of emitting transition dipoles in chlorosome from Chlorobium tepidum: fluorescence polarization anisotropy study of single chlorosomes. *Photosyn. Res.* **2009**, *100* (2), 67−78.
(186) Furumaki, S.; Vacha, F.; Habuchi, S.; Tsukatani, Y.; Bryant, D. A.; Vacha, M. Absorption Linear Dichroism Measured Directly on a Single Light-Harvesting System: The Role of Disorder in Chlorosomes of Green Photosynthetic Bacteria. *J. Am. Chem. Soc.* **2011**, *133* (17), 6703−6710.
(187) Tian, Y. X.; Camacho, R.; Thomsson, D.; Reus, M.; Holzwarth, A. R.; Scheblykin, I. G. Organization of Bacteriochlorophylls in Individual Chlorosomes from Chlorobaculum tepidum Studied by 2-Dimensional Polarization Fluorescence Microscopy. *J. Am. Chem. Soc.* **2011**, *133* (43), 17192−17199.
(188) Hoeben, F. J. M.; Jonkheijm, P.; Meijer, E. W.; Schenning, A. P. H. J. About supramolecular assemblies of pi-conjugated systems. *Chem. Rev.* **2005**, *105* (4), 1491−1546.
(189) Sundstrom, V.; Pullerits, T.; van Grondelle, R. Photosynthetic light-harvesting: Reconciling dynamics and structure of purple bacterial LH2 reveals function of photosynthetic unit. *J. Phys. Chem. B* **1999**, *103* (13), 2327−2346.
(190) van Grondelle, R.; Novoderezhkin, V. I. Energy transfer in photosynthesis: experimental insights and quantitative models. *Phys. Chem. Chem. Phys.* **2006**, *8* (7), 793−807.
(191) Jang, S. J.; Mennucci, B. Delocalized excitons in natural light-harvesting complexes. *Rev. Mod. Phys.* **2018**, *90* (3), No. 035003.
(192) Deshmukh, A. P.; Geue, N.; Bradbury, N. C.; Atallah, T. L.; Chuang, C.; Pengshung, M.; Cao, J.; Sletten, E. M.; Neuhauser, D.; Caram, J. R. Bridging the gap between H-and J-aggregates: Classification and supramolecular tunability for excitonic band structures in two-dimensional molecular aggregates. *Chem. Phys. Rev.* **2022**, *3*, No. 021401.
(193) Thilagam, A. Quantum information processing attributes of J-aggregates; *J-Aggregates, Vol. 2*, Kobayashi, T., Ed.; World Scientific: Singapore, 2012.
(194) Coles, D. M.; Meijer, A. J.; Tsoi, W. C.; Charlton, M. D.; Kim, J.-S.; Lidzey, D. G. A characterization of the Raman modes in a J-aggregate-forming dye: A comparison between theory and experiment. *J. Phys. Chem. A* **2010**, *114* (44), 11920−11927.
(195) Von Berlepsch, H.; Böttcher, C.; Ouart, A.; Burger, C.; Dähne, S.; Kirstein, S. Supramolecular structures of J-aggregates of carbocyanine dyes in solution. *J. Phys. Chem. B* **2000**, *104* (22), 5255−5262.
(196) Klymchenko, A. S. Emerging field of self-assembled fluorescent organic dye nanoparticles. *J. Nanosci. Lett.* **2013**, *3*, 21.
(197) Sung, J.; Kim, P.; Fimmel, B.; Würthner, F.; Kim, D. Direct observation of ultrafast coherent exciton dynamics in helical π-stacks of self-assembled perylene bisimides. *Nat. Commun.* **2015**, *6* (1), 8646.
(198) Kirstein, S.; Daehne, S. J-aggregates of amphiphilic cyanine dyes: Self-organization of artificial light harvesting complexes. *Int. J. Photoenergy* **2006**, *2006*, 020363.
(199) Scholes, G. D. Long-range resonance energy transfer in molecular systems. *Annu. Rev. Phys. Chem.* **2003**, *54* (1), 57−87.
(200) Longuet-Higgins, H. C. Quantum mechanics and biology. *Biophys. J.* **1962**, *2*, 207−215.
(201) Schrödinger, E. *What is Life?*; Cambridge University Press: Cambridge, 1992.
(202) Tegmark, M. Importance of quantum decoherence in brain processes. *Phys. Rev. E* **2000**, *61* (4), 4194−4206.
(203) Reimers, J. R.; McKemmish, L. K.; McKenzie, R. H.; Mark, A. E.; Hush, N. S. The revised Penrose-Hameroff orchestrated objective-reduction proposal for human consciousness is not scientifically justified Comment on "Consciousness in the universe: A review of the 'Orch OR' theory" by Hameroff and Penrose. *Phys. Life Rev.* **2014**, *11* (1), 101−103.
(204) Cogdell, R. J.; Gardiner, A. T.; Hashimoto, H.; Brotosudarmo, T. H. P. A comparative look at the first few milliseconds of the light reactions of photosynthesis. *Photochem. Photobiol. Sci.* **2008**, *7* (10), 1150−1158.
(205) Tronrud, D. E.; Wen, J.; Gay, L.; Blankenship, R. E. The structural basis for the difference in absorbance spectra for the FMO antenna protein from various green sulfur bacteria. *Photosyn. Res.* **2009**, *100*, 79−87.
(206) Maiuri, M.; Ostroumov, E. E.; Saer, R. G.; Blankenship, R. E.; Scholes, G. D. Coherent wavepackets in the Fenna−Matthews−Olson complex are robust to excitonic-structure perturbations caused by mutagenesis. *Nat. Chem.* **2018**, *10* (2), 177−183.
(207) MacColl, R.; Guard-Friar, D. *Phycobiliproteins*; CRC Press: Boca Raton, FL, 1987.
(208) Glazer, A. N.; Wedemayer, G. J. Cryptomonad biliproteins—an evolutionary perspective. *Photosyn. Res.* **1995**, *46*, 93−105.
(209) Blankenship, R. E. *Molecular Mechansims of Photosynthesis*; Blackwell Science: Oxford, 2002.
(210) Jumper, C. C.; Van Stokkum, I. H.; Mirkovic, T.; Scholes, G. D. Vibronic wavepackets and energy transfer in cryptophyte light-harvesting complexes. *J. Phys. Chem. B* **2018**, *122* (24), 6328−6340.
(211) Marin, A.; Doust, A. B.; Scholes, G. D.; Wilk, K. E.; Curmi, P. M.; Van Stokkum, I. H.; Van Grondelle, R. Flow of excitation energy in the cryptophyte light-harvesting antenna phycocyanin 645. *Biophys. J.* **2011**, *101* (4), 1004−1013.
(212) McClure, S. D.; Turner, D. B.; Arpin, P. C.; Mirkovic, T.; Scholes, G. D. Coherent oscillations in the PC577 cryptophyte antenna occur in the excited electronic state. *J. Phys. Chem. B* **2014**, *118* (5), 1296−1308.
(213) Arpin, P. C.; Turner, D. B.; McClure, S. D.; Jumper, C. C.; Mirkovic, T.; Challa, J. R.; Lee, J.; Teng, C. Y.; Green, B. R.; Wilk, K. E.; et al. Spectroscopic studies of cryptophyte light harvesting proteins: Vibrations and coherent oscillations. *J. Phys. Chem. B* **2015**, *119* (31), 10025−10034.
(214) Harrop, S. J.; Wilk, K. E.; Dinshaw, R.; Collini, E.; Mirkovic, T.; Teng, C. Y.; Oblinsky, D. G.; Green, B. R.; Hoef-Emden, K.; Hiller, R. G.; et al. Single-residue insertion switches the quaternary structure and exciton states of cryptophyte light-harvesting proteins. *Proc. Natl. Acad. Sci. U.S.A.* **2014**, *111* (26), E2666−E2675.
(215) Dean, J. C.; Mirkovic, T.; Toa, Z. S.; Oblinsky, D. G.; Scholes, G. D. Vibronic enhancement of algae light harvesting. *Chem.* **2016**, *1* (6), 858−872.
(216) Roy, P. P.; Leonardo, C.; Orcutt, K.; Oberg, C.; Scholes, G. D.; Fleming, G. R. Infrared Signatures of Phycobilins within the Phycocyanin 645 Complex. *J. Phys. Chem. B* **2023**, *127* (20), 4460−4469.
(217) Gantt, E. Phycobilisomes: Light-harvesting pigment complexes. *Bioscience* **1975**, *25* (12), 781−788.
(218) Glazer, A. N. Light harvesting by phycobilisomes. *Annu. Rev. Biophys.* **1985**, *14* (1), 47−77.
(219) David, L.; Marx, A.; Adir, N. High-resolution crystal structures of trimeric and rod phycocyanin. *J. Mol. Biol.* **2011**, *405* (1), 201−213.
(220) Rosinski, J.; Hainfeld, J.; Rigbi, M.; Siegelman, H. Phycobilisome ultrastructure and chromatic adaptation in Fremyella diplosiphon. *Ann. Bot.* **1981**, *47* (1), 1−12.

https://doi.org/10.1021/acs.jpclett.4c00264
J. Phys. Chem. Lett. 2024, 15, 3294−3316

(221) Sil, S.; Tilluck, R. W.; Mohan TM, N.; Leslie, C. H.; Rose, J. B.; Domínguez-Martín, M. A.; Lou, W.; Kerfeld, C. A.; Beck, W. F. Excitation energy transfer and vibronic coherence in intact phycobilisomes. *Nat. Chem.* **2022**, *14* (11), 1286−1294.
(222) Sener, M.; Strumpfer, J.; Timney, J. A.; Freiberg, A.; Hunter, C. N.; Schulten, K. Photosynthetic vesicle architecture and constraints on efficient energy harvesting. *Biophys. J.* **2010**, *99* (1), 67−75.
(223) Kosztin, I.; Schulten, K. Structure, function, and quantum dynamics of pigment−protein complexes. *Quantum Effects in Biology* **2014**, 123.
(224) Sener, M.; Strumpfer, J.; Hsin, J.; Chandler, D.; Scheuring, S.; Hunter, C. N.; Schulten, K. Forster Energy Transfer Theory as Reflected in the Structures of Photosynthetic Light-Harvesting Systems. *ChemPhysChem* **2011**, *12* (3), 518−531.
(225) Scholes, G. D.; Fleming, G. R. On the mechanism of light harvesting in photosynthetic purple bacteria: B800 to B850 energy transfer. *J. Phys. Chem. B* **2000**, *104* (8), 1854−1868.
(226) Gabrielsen, M.; Gardiner, A. T.; Cogdell, R. J. *The Purple Phototrophic Bacteria: Advances in Photosynthesis and Respiration*; Springer: Dordrecht, The Netherlands, 2008.
(227) Reddy, K. R.; Jiang, J. B.; Krayer, M.; Harris, M. A.; Springer, J. W.; Yang, E.; Jiao, J. Y.; Niedzwiedzki, D. M.; Pandithavidana, D.; Parkes-Loach, P. S.; Kirmaier, C.; Loach, P. A.; Bocian, D. F.; Holten, D.; Lindsey, J. S. Palette of lipophilic bioconjugatable bacteriochlorins for construction of biohybrid light-harvesting architectures. *Chem. Sci.* **2013**, *4* (5), 2036−2053.
(228) Koepke, J.; Hu, X. C.; Muenke, C.; Schulten, K.; Michel, H. The crystal structure of the light-harvesting complex II (B800−850) from Rhodospirillum molischianum. *Structure* **1996**, *4* (5), 581−597.
(229) Papiz, M. Z.; Prince, S. M.; Howard, T.; Cogdell, R. J.; Isaacs, N. W. The structure and thermal motion of the B800−850 LH2 complex from Rps.acidophila at 2.0A resolution and 100K: new structural features and functionally relevant motions. *J. Mol. Biol.* **2003**, *326* (5), 1523−1538.
(230) Pullerits, T.; Chachisvilis, M.; Sundström, V. Exciton delocalization length in the B850 antenna of Rhodobacter sphaeroides. *J. Phys. Chem.* **1996**, *100* (25), 10787−10792.
(231) Yang, C.; Zhang, W.; Pang, X.; Xiao, F.; Kalva, S.; Zhang, Y.; Pramanik, M.; Tian, L.; Liu, G.; Wang, M. Polyester-tethered near-infrared fluorophores confined in colloidal nanoparticles: Tunable and thermoresponsive aggregation and biomedical applications. *Aggregate* **2023**, *4* (2), No. e261.
(232) Kirchner, E.; Bialas, D.; Fennel, F.; Grune, M.; Wurthner, F. Defined Merocyanine Dye Stacks from a Dimer up to an Octamer by Spacer-Encoded Self-Assembly Approach. *J. Am. Chem. Soc.* **2019**, *141* (18), 7428−7438.
(233) Gorman, J.; Orsborne, S. R. E.; Sridhar, A.; Pandya, R.; Budden, P.; Ohmann, A.; Panjwani, N. A.; Liu, Y.; Greenfield, J. L.; Dowland, S.; Gray, V.; Ryan, S. T. J.; De Ornellas, S.; El-Sagheer, A. H.; Brown, T.; Nitschke, J. R.; Behrends, J.; Keyser, U. F.; Rao, A.; Collepardo-Guevara, R.; Stulz, E.; Friend, R. H.; Auras, F. Deoxyribonucleic Acid Encoded and Size-Defined pi-Stacking of Perylene Diimides. *J. Am. Chem. Soc.* **2022**, *144* (1), 368−376.
(234) Eisele, D. M.; Berlepsch, H. V.; Bottcher, C.; Stevenson, K. J.; Vanden Bout, D. A.; Kirstein, S.; Rabe, J. P. Photoinitiated Growth of Sub-7 nm Silver Nanowires within a Chemically Active Organic Nanotubular Template. *J. Am. Chem. Soc.* **2010**, *132* (7), 2104−2105.
(235) Eisele, D. M.; Cone, C. W.; Bloemsma, E. A.; Vlaming, S. M.; van der Kwaak, C. G. F.; Silbey, R. J.; Bawendi, M. G.; Knoester, J.; Rabe, J. P.; Vanden Bout, D. A. Utilizing redox-chemistry to elucidate the nature of exciton transitions in supramolecular dye nanotubes. *Nat. Chem.* **2012**, *4* (8), 655−662.
(236) Fidder, H.; Knoester, J.; Wiersma, D. A. Optical-Properties of Disordered Molecular Aggregates - a Numerical Study. *J. Chem. Phys.* **1991**, *95* (11), 7880−7890.
(237) Eisfeld, A.; Briggs, J. S. The J-band of organic dyes: lineshape and coherence length. *Chem. Phys.* **2002**, *281* (1), 61−70.
(238) Eisele, D. M.; Arias, D. H.; Fu, X. F.; Bloemsma, E. A.; Steiner, C. P.; Jensen, R. A.; Rebentrost, P.; Eisele, H.; Tokmakoff, A.; Lloyd, S.; Nelson, K. A.; Nicastro, D.; Knoester, J.; Bawendi, M. G. Robust excitons inhabit soft supramolecular nanotubes. *Proc. Natl. Acad. Sci. U.S.A.* **2014**, *111* (33), E3367−E3375.
(239) Kriete, B.; Luttig, J.; Kunsel, T.; Maly, P.; Jansen, T. L. C.; Knoester, J.; Brixner, T.; Pshenichnikov, M. S. Interplay between structural hierarchy and exciton diffusion in artificial light harvesting. *Nat. Commun.* **2019**, *10* (1), 4615.
(240) Caram, J. R.; Doria, S.; Eisele, D. M.; Freyria, F. S.; Sinclair, T. S.; Rebentrost, P.; Lloyd, S.; Bawendi, M. G. Room-Temperature Micron-Scale Exciton Migration in a Stabilized Emissive Molecular Aggregate. *Nano Lett.* **2016**, *16* (11), 6808−6815.
(241) Qiao, Y.; Polzer, F.; Kirmse, H.; Steeg, E.; Kuhn, S.; Friede, S.; Kirstein, S.; Rabe, J. P. Nanotubular J-Aggregates and Quantum Dots Coupled for Efficient Resonance Excitation Energy Transfer. *ACS Nano* **2015**, *9* (2), 1552−1560.
(242) Herman, K.; Kirmse, H.; Eljarrat, A.; Koch, C. T.; Kirstein, S.; Rabe, J. P. Individual tubular J-aggregates stabilized and stiffened by silica encapsulation. *Colloid Polym. Sci.* **2020**, *298* (7), 937−950.
(243) Ng, K.; Webster, M.; Carbery, W. P.; Visaveliya, N.; Gaikwad, P.; Jang, S. J.; Kretzschmar, I.; Eisele, D. M. Frenkel excitons in heat-stressed supramolecular nanocomposites enabled by tunable cage-like scaffolding. *Nat. Chem.* **2020**, *12* (12), 1157−1164.
(244) Qiao, Y.; Polzer, F.; Kirmse, H.; Kirstein, S.; Rabe, J. P. Nanohybrids from nanotubular J-aggregates and transparent silica nanoshells. *Chem. Commun.* **2015**, *51* (60), 11980−11982.
(245) Zhang, Y.; Lou, H.; Zhang, W.; Wang, M. Mussel-Inspired Surface Coating to Stabilize and Functionalize Supramolecular J-Aggregate Nanotubes Composed of Amphiphilic Cyanine Dyes. *Langmuir* **2022**, *38* (26), 8160−8168.
(246) Wittmann, B.; Wenzel, F. A.; Wiesneth, S.; Haedler, A. T.; Drechsler, M.; Kreger, K.; Kohler, J.; Meijer, E. W.; Schmidt, H. W.; Hildner, R. Enhancing Long-Range Energy Transport in Supramolecular Architectures by Tailoring Coherence Properties. *J. Am. Chem. Soc.* **2020**, *142* (18), 8323−8330.
(247) Bredas, J. L.; Sargent, E. H.; Scholes, G. D. Photovoltaic concepts inspired by coherence effects in photosynthetic systems. *Nat. Mater.* **2017**, *16* (1), 35−44.
(248) Fassioli, F.; Dinshaw, R.; Arpin, P. C.; Scholes, G. D. Photosynthetic light harvesting: excitons and coherence. *J. R. Soc. Interface* **2014**, *11* (92), No. 20130901.
(249) Lin, J. D. A.; Mikhnenko, O. V.; Chen, J. R.; Masri, Z.; Ruseckas, A.; Mikhailovsky, A.; Raab, R. P.; Liu, J. H.; Blom, P. W. M.; Loi, M. A.; Garcia-Cervera, C. J.; Samuel, I. D. W.; Nguyen, T. Q. Systematic study of exciton diffusion length in organic semiconductors by six experimental methods. *Mater. Horizons* **2014**, *1* (2), 280−285.
(250) Menke, S. M.; Holmes, R. J. Exciton diffusion in organic photovoltaic cells. *Energy Environ. Sci.* **2014**, *7* (2), 499−512.
(251) Haedler, A. T.; Kreger, K.; Issac, A.; Wittmann, B.; Kivala, M.; Hammer, N.; Kohler, J.; Schmidt, H. W.; Hildner, R. Long-range energy transport in single supramolecular nanofibres at room temperature. *Nature* **2015**, *523* (7559), 196−199.
(252) Haedler, A. T.; Beyer, S. R.; Hammer, N.; Hildner, R.; Kivala, M.; Kohler, J.; Schmidt, H. W. Synthesis and Photophysical Properties of Multichromophoric Carbonyl-Bridged Triarylamines. *Chem.—Eur. J.* **2014**, *20* (37), 11708−11718.
(253) Saikin, S. K.; Shakirov, M. A.; Kreisbeck, C.; Peskin, U.; Proshin, Y. N.; Aspuru-Guzik, A. On the Long-Range Exciton Transport in Molecular Systems: The Application to H-Aggregated Heterotriangulene Chains. *J. Phys. Chem. C* **2017**, *121* (45), 24994−25002.
(254) Wang, M.; Zhang, Y.; Zhang, W. Bioinspired molecular qubits and nanoparticle ensembles that could be initialized, manipulated and readout under mild conditions. *J. Phys. Chem. Lett.* **2022**, *13* (2), 508−513.
(255) Thilagam, A. Entanglement dynamics of J-aggregate systems. *J. Phys. A Math. Theor.* **2011**, *44* (13), 135306.
(256) Thilagam, A. Grover-like search via a Frenkel-exciton trapping mechanism. *Phys. Rev. A* **2010**, *81* (3), 032309.

https://doi.org/10.1021/acs.jpclett.4c00264
J. Phys. Chem. Lett. 2024, 15, 3294−3316

(257) Kong, F. F.; Tian, X. J.; Zhang, Y.; Zhang, Y.; Chen, G.; Yu, Y. J.; Jing, S. H.; Gao, H. Y.; Luo, Y.; Yang, J. L.; Dong, Z. C.; Hou, J. G. Wavelike electronic energy transfer in donor-acceptor molecular systems through quantum coherence. *Nat. Nanotechnol.* **2022**, *17* (17), 729−736.
(258) Zhang, Y.; Luo, Y.; Zhang, Y.; Yu, Y. J.; Kuang, Y. M.; Zhang, L.; Meng, Q. S.; Luo, Y.; Yang, J. L.; Dong, Z. C.; Hou, J. G. Visualizing coherent intermolecular dipole-dipole coupling in real space. *Nature* **2016**, *531* (7596), 623−627.
(259) Gabas, F.; Di Liberto, G.; Conte, R.; Ceotto, M. Protonated glycine supramolecular systems: the need for quantum dynamics. *Chem. Sci.* **2018**, *9* (41), 7894−7901.
(260) Kundu, S.; Makri, N. Exciton−vibration dynamics in J-aggregates of a perylene bisimide from real-time path integral calculations. *J. Phys. Chem. C* **2021**, *125* (1), 201−210.
(261) Kirchner, E.; Bialas, D.; Fennel, F.; Grune, M.; Würthner, F. Defined Merocyanine Dye Stacks from a Dimer up to an Octamer by Spacer-Encoded Self-Assembly Approach. *J. Am. Chem. Soc.* **2019**, *141* (18), 7428−7438.

https://doi.org/10.1021/acs.jpclett.4c00264
J. Phys. Chem. Lett. 2024, 15, 3294−3316